

1 **A new habitat map of the Lena Delta in Arctic Siberia**
2 **based on field and remote sensing datasets**

3 Simeon Lisovski^{1,*}, Alexandra Runge^{2,*}, Iuliia Shevtsova¹, Nele Landgraf³, Anne Morgenstern²,
4 Ronald Reagan Okoth^{1,4}, Matthias Fuchs², Nikolay Lashchinskiy^{5,6}, Carl Stadie^{2,7}, Alison
5 Beamish⁸, Ulrike Herzs Schuh^{1,9,10}, Guido Grosse^{1,11}, Birgit Heim¹

6

7 * Both authors contributed equally

8 ¹ Alfred Wegener Institute Helmholtz Centre for Polar and Marine Research, Polar Terrestrial
9 Environmental Systems, 14473 Potsdam, Germany

10 ² Alfred Wegener Institute Helmholtz Centre for Polar and Marine Research, Permafrost Research, 14473
11 Potsdam, Germany

12 ³ Humboldt University, Department of Geosciences, 12489 Berlin, Germany

13 ⁴ Julius-Maximilians Universität Würzburg, Institute of Geography and Geology, Oswald-Külpe-Weg 86,
14 97074 Würzburg, Germany

15 ⁵ Central Siberian Botanical Garden, Siberian Branch, Russian Academy of Sciences, Novosibirsk,
16 630090 Russia

17 ⁶ Trofimuk Institute of Petroleum Geology and Geophysics, Siberian Branch, Russian Academy of
18 Sciences, Novosibirsk, 630090 Russia

19 ⁷ University of Greifswald, Institute for Geography and Geology, Germany (current address: University of
20 Copenhagen, Department of Earth Science and Nature Management, Denmark)

21 ⁸ GFZ German Research Centre for Geosciences, Helmholtz Centre Potsdam.

22 ⁹ University of Potsdam, Institute of Environmental Sciences & Geography, Karl-Liebknecht-Str. 24-25,
23 14476 Potsdam, Germany

24 ¹⁰ University of Potsdam, Institute of Biochemistry and Biology, Karl-Liebknecht-Str. 24-25, 14476
25 Potsdam, Germany

26 ¹¹ University of Potsdam, Institute of Geosciences, Karl-Liebknecht-Str. 24-25, 14476 Potsdam, Germany

27 *Correspondence to:* Simeon Lisovski (Simeon.Lisovski@awi.de), Alexandra Runge
28 (alexandra.runge@gfz-potsdam.de), Birgit Heim (birgit.heim@awi.de)

29

30 **Abstract.** The Lena Delta is the largest river delta in the Arctic (about 30 000 km²) and prone to
31 rapid changes due to climate warming, associated cryosphere loss and ecological shifts. The delta is
32 characterized by ice-rich permafrost landscapes and consists of geologically and geomorphologically
33 diverse terraces covered with tundra vegetation and of active floodplains, featuring approximately 6
34 500 km of channels and over 30 000 lakes. Because of its broad landscape and habitat diversity the
35 delta is a biodiversity hotspot with high numbers of nesting and breeding migratory birds, fish,
36 caribou and other mammals and was designated a State Nature Reserve in 1995. Characterizing
37 plant composition, above ground biomass and application of field spectroscopy was a major focus of
38 a 2018 expedition to the delta. These field data collections were linked to Sentinel-2 satellite data to
39 upscale local patterns in land cover and associated habitats to the entire delta. Here, we describe
40 multiple field datasets collected in the Lena Delta during summer 2018 including foliage projective
41 cover (Shevtsova et al., 2021a), above ground biomass (Shevtsova et al., 2021b), and hyperspectral
42 field measurements (Runge et al., 2022, <https://doi.pangaea.de/10.1594/PANGAEA.945982>). We
43 further describe a detailed Sentinel-2 satellite image-based classification of habitats for the central
44 Lena Delta (Landgraf et al., 2022), an upscaled classification for the entire Lena Delta (Lisovski et
45 al., 2022), as well as a synthesis product for disturbance regimes (Heim and Lisovski, 2023,
46 <https://doi.org/10.5281/zenodo.7575691>) in the delta that is based on the classification, the
47 described datasets, and field expertise. We present context and detailed methods of these openly
48 available datasets and show how their combined use can improve our understanding of the rapidly
49 changing Arctic tundra system. The new Lena Delta habitat classification represents a first baseline
50 against which future observations can be compared. The link between such detailed habitat
51 classifications and disturbance regime may provide a better understanding of how Arctic lowland
52 landscapes will respond to climate change and how this will impact land surface processes.

53

54 1 Introduction

55 Global warming has profound impacts on the polar regions (Serreze and Barry, 2011; Overland et
56 al., 2019). Rapidly increasing temperatures and changing precipitation regimes result in declining
57 sea ice, warming and thawing of permafrost, more frequent tundra fires, and changes in vegetation
58 (e.g., Biskaborn et al., 2019; Hu et al., 2015; Mauclet et al., 2022; Box et al., 2019; Amap, 2021).
59 The Arctic tundra biome, which is normally characterized by harsh living conditions and nutrient-
60 deficiency, has experienced rapid phenological shifts, such as earlier green-up in spring, which is
61 also associated with increasing shrubification rates (Mekonnen et al., 2021). Shifts in plant
62 communities are also driven by changing nutrient availability in permafrost soils (Mekonnen et al.,
63 2021; Mauclet et al., 2022), affecting the net primary productivity of tundra ecosystems.

64 Satellite-derived remote sensing can provide large-scale assessments of Arctic vegetation cover and
65 changes therein (Bartsch et al., 2016). For example, the Circumpolar Arctic Vegetation Map (CAVM)
66 project, from the Conservation of Arctic Flora and Fauna working group (CAFF), provided a first
67 panarctic vegetation composition map based on Advanced Very-High Resolution Radiometer
68 (AVHRR) false-color infrared (CIR) composites at a 1:4 million map scale (Walker, 1998; Raynolds
69 et al., 2019). Later, higher resolution land cover maps became available across all spatial scales
70 from national and international efforts such as the NASA Arctic-Boreal Vulnerability Experiment
71 (ABoVE) providing open-source data collections from boreal and arctic regions (ABoVE Science
72 Definition Team, 2014) specifically for Alaska, Canada, Northern Europe, and Western Siberia,
73 providing a better bridge to field measurements. Such products greatly assist in monitoring and
74 upscaling of patterns and dynamics of soil properties, land-atmosphere fluxes, ecosystem states,
75 and changes therein (e.g., Walker, 1998; Beamish et al., 2020; Berner et al., 2020; Sweeney et al.,
76 2022; Macander et al., 2022; Endsley et al., 2022). For selected Eastern Siberian tundra regions,
77 land cover maps have been produced (e.g., Veremeeva and Gubin, 2009; Bartsch et al., 2019;
78 Schneider et al., 2009), including the Lena Delta (Bartsch et al., 2019; Schneider et al., 2009).

79 Arctic river deltas represent distinct and vulnerable geomorphological and ecological regions at the
80 marine-terrestrial boundary. River deltas have been studied intensively to better understand land
81 cover and vegetation compositions (Jorgenson, 2000; Schneider et al., 2009; Frost et al., 2020;
82 Bartsch et al., 2020), carbon pools and fluxes (Bartlett et al., 1992; Schneider et al., 2009; Sachs et
83 al., 2008; Rossgger et al., 2022), and land cover change caused by climate change impacts
84 (Jorgenson, 2000; Pizaric et al., 2011; Lantz et al., 2015; Nitze and Grosse, 2016; Vulis et al., 2021;
85 Juhls et al., 2021). With diverse habitats, Arctic river deltas are biodiversity hotspots (Gilg et al.,
86 2000), but at the same time are prone to rapid changes (Walker, 1998; Overeem et al., 2022). Arctic

87 deltas are affected by permafrost thaw (e.g., Pizaric et al., 2011; Nitze and Grosse, 2016; Vulis et
88 al., 2021), sea ice loss (Overeem et al., 2022), and increased sediment transport and organic load
89 during spring floods (Piliouras and Rowland, 2020; Juhls et al., 2021). Arctic river deltas are very
90 dynamic systems and high-resolution habitat information from these biodiversity hotspots is needed
91 to assess and predict changes and implications of Arctic warming.

92 The Lena Delta is the largest Arctic river delta representing a typical lake-rich lowland permafrost
93 landscape (Grigoriev, 1993). Over the past decades, the central Lena Delta became a place of
94 intensive international research. In addition to long-term permafrost monitoring at the Research
95 Station Samoylov Island (Hubberten et al., 2006; Boike et al., 2019), extensive records on
96 meteorology, soil and ecosystem characteristics (Zibulski et al., 2016; Boike et al., 2019; Boike et al.,
97 2008), hydrology (Fedorova et al., 2015), and greenhouse gas fluxes (Rossgger et al., 2022; Holl et
98 al., 2019) are available, setting an important benchmark for further assessments of changes in an
99 Arctic river delta. During the summer season of 2018, an extensive field campaign to the Lena Delta
100 led to an unprecedented amount of field datasets including vegetation cover recordings, above
101 ground biomass estimates, and spectral characterisation of the different vegetation/land cover units.
102 These in situ datasets provide improved thematic detail allowing the development of habitat
103 classifications. In 2009, Schneider et al. (2009) developed the first land cover classification map for
104 the entire delta at 30 m spatial resolution based on Landsat-7 ETM+ satellite summer images from
105 2000 and 2001 to quantify delta-wide methane emissions. The availability of Sentinel-2 ([Sentinel-2](#))
106 Multispectral Instrument (MSI) data from two orbiting satellite missions since 2016 and 2017 provide
107 high quality multispectral satellite data with a higher spatial resolution in the Visible and Near
108 Infrared wavelength of up to 10 m, and of 20 m in the Red Edge and the Short- Wave Infrared
109 wavelength regions (Drusch et al., 2012, ESA 2015). Together with the extensive ground
110 observations from the Lena Delta in 2018 this enables an updated classification, using the higher
111 resolution [Sentinel-2](#) images and improved thematic detail.

Deleted: S-2

Deleted: S-2

112 In the following study, field datasets as well as derived multispectral satellite images from the
113 summer season 2018 for the Lena Delta were used to provide 1) an updated data-driven framework
114 for plant communities and associated habitat classes in the Lena Delta, 2) a high-resolution habitat
115 mapping product for the entire delta, and 3) a disturbance regime map linked to habitat classes.
116 These datasets enhance our understanding of the Lena Delta system and will build a baseline and
117 framework for future spatio-temporal analysis of more detailed processes and changes within this
118 highly sensitive ecosystem.

121 2 Study Area

122 The Lena Delta is located in northeastern Siberia's continuous permafrost zone between 72° and
123 74°N and 123° to 130°E (Figure 1). With an area of about 30 000 km², it is the largest delta in the
124 Arctic and one of the largest in the world (Walker, 1998; Schneider et al., 2009). It is surrounded by
125 the Laptev Sea to the west, north, and east, and the Chekanovsky and Kharaulakh mountain ranges
126 border it to the south. The delta is characterized by numerous river channels and more than 1500
127 islands with a diverse geologic history (Grigoriev, 1993). Morphologically, the delta can be divided
128 into three distinct geomorphological main terraces (Grigoriev, 1993; Schwamborn et al., 2002). The
129 first main terrace, which comprises the Holocene fluvial terraces and the active floodplains, is the
130 youngest and most active part of the delta (Schwamborn et al., 2023), and covers most of the east-
131 northeastern areas as well as the southern and southwestern-most parts. This main terrace
132 predominantly consists of ice wedge-polygonal tundra (Nitzbon et al., 2020) as well as of barren and
133 vegetated floodplain areas (e.g., Rossger et al., 2022). The second main terrace, located in the
134 northwestern part, contains mostly sandy, comparably well-drained soils with low ground-ice content
135 (Schwamborn et al., 2002; Ulrich et al., 2009). Large, mostly north-to-south oriented lakes and
136 depressions are abundant in this area (Morgenstern et al., 2008). The third and oldest main terrace
137 consists mainly of remnants of a Late Pleistocene accumulation plain with ice- and organic-rich
138 sediments (so-called Yedoma deposits) and is characterized by polygonal tundra with large ice
139 wedges, deep thermokarst lake basins, and thermo-erosional valleys (Morgenstern et al., 2011;
140 Morgenstern et al., 2021). The third terrace is found on islands in the southern delta region
141 (Schirrmeister et al., 2003; Schirrmeister et al., 2011). Permafrost in the area has a thickness of
142 about 500–600 m (Romanovskii and Hubberten, 2001). The active layer depth, i.e., the seasonally
143 thawing upper soil layer, on the first terrace is usually in the range of 30 to 50 cm and 80 to 120 cm
144 on the floodplains (Boike et al., 2019). The larger region is characterized by an Arctic continental
145 climate with low mean annual air temperatures of –13 °C, a mean temperature in January of –32 °C,
146 and a mean temperature in July of 6.5 °C. The mean annual precipitation is low and amounts to
147 about 190 mm (World Weather Information Service).

148 As part of past Russian-German expeditions to the Lena Delta, most research during the last two
149 decades has been carried out on the islands of Samoylov and Kurungnakh in the central delta
150 (Figure 1). Samoylov Island (72°22' N, 126°29' E) covers an area of about 5 km² and is
151 representative of the first terrace together with an active floodplain (Boike et al., 2019; Boike et al.,
152 2008). The vegetation and soil types are diverse at local scales due to high lateral variability of the
153 polygonal microrelief consisting of drier polygon rims, and moist to wet polygonal depressions and
154 troughs (Nitzbon et al., 2020; Kienast and Tsherkasova, 2001). In contrast, Kurungnakh Island is

155 mainly composed of late Pleistocene Yedoma deposits that belong to the third delta terrace
156 (Grigoriev, 1993) with elevation up to 55 m above sea level (m a.s.l.) (Morgenstern et al., 2013).
157 Holocene cover deposits and peat-rich permafrost soils are distributed across the surface of the third
158 Lena River terrace and especially concentrated in the deep thermokarst basins called “alases”.
159 Alases are important landscape-forming features of the ice-rich Yedoma permafrost zone, which are
160 mainly caused by extensive melting of excess ground ice in the underlying permafrost (Van
161 Everdingen, 1998).

162

163 3 Datasets and methods

164 Several new datasets are presented for the Lena Delta that are spatially and thematically connected
165 and support vegetation, habitat, and land cover applications for this region (Figure 1).

166 Two datasets feature field-measured vegetation data, providing information on foliage projective
167 cover (Dataset 1) and above ground biomass (Dataset 2) recorded in the central Lena Delta in
168 summer 2018 across 26 selected vegetation plot sites (supplementary table S1, S2). The field plots
169 of 30 x 30 m (900 m²) were chosen to be representative for typical vegetation communities (vascular
170 plants, moss and lichen cover) as largely homogenous sites representative for the surrounding area.
171 In addition, a total of 28 in-situ, canopy-level hyperspectral field measurements were acquired in 30
172 x 30 m plots with homogeneous vegetation or barren to partially vegetated areas (spectral
173 reflectance field measurements; Dataset 3). Of the 28 hyperspectral measurements, 15 were
174 conducted at the vegetation plot sites of Datasets 1,2 three measurements were repeat
175 measurements to capture vegetation senescence, and at 10 spectrometry plots we conducted
176 hyperspectral field measurements without floristic inventories but with detailed plot documentation.
177 Based on expert knowledge, we defined representative habitat classes and identified homogeneous
178 regions within the central Lena Delta to train and apply a classifier using a [Sentinel-2](#) satellite image
179 from summer 2018 (Dataset 4). Due to the high reliability of the central Lena Delta vegetation
180 classification and positive evaluation by field experts, we used this vegetation classification as a
181 training dataset for a robust classifier that was subsequently applied to a [Sentinel-2](#) image mosaic
182 for the entire Lena Delta for 2018 to develop a new Lena Delta habitat map (Dataset 5).

Deleted: S-2

Deleted: S-2

183 Finally, using the habitat classes, probability maps for exposed sandbars and water distribution, and
184 information from the in-situ dataset (Datasets 1 & 2), we extrapolated a classification of disturbance
185 regimes across the delta (Dataset 6) as an application example for the habitat classes.

188 **3.1 Foliage projective cover (Dataset 1)**

189 A detailed description of plant composition for the 26 vegetation plots of the 2018 expedition to the
190 Lena Delta was compiled (see supplementary table S1, S2, S3). Prior to the field work, the
191 approximate site locations were defined for establishing representative vegetation plots based on
192 field knowledge and evaluation of Landsat and Sentinel-2 satellite imagery. The aim was to cover
193 representative vegetation communities of the central delta. There are vegetation communities with
194 large area coverage that show high homogeneity within larger areas (10s of meters). Therefore, at
195 each site location, we defined a 30 x 30 m square plot with a homogeneous or repetitive vegetation
196 composition that was also representative of the wider land surface serving as an Elementary
197 Sampling Unit (ESU). ESUs according to the Committee on Earth Observing Satellites Working
198 Group on Calibration and Validation (Duncanson et al., 2021) serve as spatial training and
199 validation units representative for the land surface for quantitative and qualitative remote
200 sensing operations. In case of more patchy and heterogeneous vegetation structure we selected 30
201 x 30 m squares embedded in a minimum of 50 x 50 m square of the same vegetation composition.

202 The detailed floristic composition was recorded around the plot center in four successive rings of 50
203 cm diameter. In addition, the vegetation plot was mapped in detail from above with one Red-Green-
204 Blue (RGB) and one Red-Green-Near Infrared (RGNIR) MAPIR camera using telescope stick-based
205 field photography. The projective vegetation cover was recorded in at least three subplots (2 m x 2
206 m) within the plot. If the vegetation cover was highly homogenous three subplots were established.
207 In the case of moisture differences, e.g. in polygonal tundra with dry rims and moist to wet
208 depressions, we established higher numbers of subplots capturing moist as well as dry patches
209 (see, Figure 2 & 3 describing the concept). We compiled the floristic composition to foliage projective
210 cover by plant taxa on each 2 x 2 m subplot for the different canopy levels and extrapolated for the
211 30 m x 30 m plot. We used the RGB and NIR field photos to make an estimate on the share of moist
212 and dry surface area to calculate an averaged projective vegetation cover. The ring survey data was
213 not included in the plot average. The dataset of percentage foliage projective cover per vegetation
214 plot is published in PANGAEA (Shevtsova et al., 2021a,
215 <https://doi.pangaea.de/10.1594/PANGAEA.935875>).

216 **3.2 Above ground plant biomass (Dataset 2)**

217 Above-ground biomass (ABG) was sampled in the field in 25 of the 26 vegetation plots in 2018 (see
218 supplementary table S1, S2, S3). Within each 2 x 2 m subplot a 0.5 m x 0.5 m representative plot

219 was selected for ABG sampling. AGB sampling for moss and lichens was conducted within 0.1 m x
220 0.1 m subplots inside the 0.5 m x 0.5 m subplots.

221 In total, 174 fresh AGB samples were collected and weighed in the field or subsequently at the
222 Samoylov research station. AGB samples with a weight exceeding 15 g were subsampled. The plant
223 samples were then dried for two to four days in a warm dry place and finally oven-dried for ca. 24
224 hours at a temperature of 60 °C before re-weighing. All AGB assessments per plant community type
225 were upscaled to the 30 m x 30 m plot in g/m² using the foliage projective cover data. The dataset of
226 AGB per vegetation plot has been published in PANGAEA (Shevtsova et al., 2021b,
227 <https://doi.pangaea.de/10.1594/PANGAEA.935923>).

228 **3.3 Hyperspectral field measurements (Dataset 3)**

229 Hyperspectral field measurements were conducted in the central Lena Delta in August 2018 with the
230 aim to collect surface reflectance spectra of different homogeneous land cover units across a variety
231 of delta land surfaces and vegetation composition. In total, we collected 28 hyperspectral field
232 measurements in homogeneous 30 x 30 m spectrometry plots (Table S5), with 15 of them equalling
233 the vegetation plots across Samoylov and Kurungnakh islands (see Dataset 1 & 2 and
234 *supplementary table S4*), three as repeat measurements at the end of August to capture the change
235 in spectral signature during senescence since the beginning of August and the remaining 10 field-
236 spectroscopy plots focusing on non-vegetated areas such as sandy parts of the floodplain. We
237 conducted the field-spectroscopy measurements with a Spectral Evolution SR-2500 field
238 spectrometer with a 1.5 m Fiber Optic Cable. The instrument was calibrated to spectral radiance
239 within a wavelength range of 350 to 2500 nm. Within the 30 x 30 m homogeneous spectrometry
240 plots we acquired about 100 individual measurements, randomly scattered across the plot. Before
241 and after each survey we conducted reference measurements by measuring the back reflected
242 downwelling radiance from a Zenith Lite™ Diffuse Reflectance Target of 50% reflectivity to normalize
243 to surface reflectance percentages per wavelength. The averaged individual measurements of the
244 reflectance of each spectrometry plot was published in the PANGAEA data repository (Runge et al.,
245 2022, <https://doi.pangaea.de/10.1594/PANGAEA.945982>).

246 **3.4 Central Lena Delta habitat classification (Dataset 4)**

247 *3.4.1 Habitat classes*

248 Based on the vegetation plots (Dataset 1 & 2) and from field knowledge, different habitat classes
249 characterized by distinct plant communities, moisture regimes and soil properties were defined. Non-

250 vegetated areas (e.g., sand) and water were added as additional classes using band thresholds
251 (Table 1). During an iterative process within a Sentinel-2 based supervised classification, additional
252 habitat classes that were not covered by the vegetation plots (Dataset 1 & 2) were added: i) The
253 polygonal tundra complex could spectrally be separated into distinct classes related to different
254 surface water abundance in the form of intra- and interpolygonal ponds, therefore, we implemented
255 three different polygonal tundra complex classes, with up to 10%, 20%, 50% surface water cover
256 respectively, and ii) one class of 'sparsely vegetated' representing the areas of transition zones
257 between vegetated and barren. Table 1 provides details on habitat class descriptions and
258 established methods to distinguish habitats.

Deleted: S-2

259 3.4.2 Satellite data processing

260 The central Lena Delta habitat classification is based on one high quality cloudless Sentinel-2
261 image from August 6 in 2018, representing the late summer. The Sentinel-2 top of atmosphere
262 reflectance (TOA) image data was processed by the German Space Agency DLR (B. Pflug, oral
263 communication, 2019) to bottom of atmosphere (BOA) surface reflectance using the newest version
264 of the atmospheric correction processor Sen2Cor later released as ESA Sen2Cor in 2020.
265 Atmospheric correction processing was performed with the default rural aerosol model. All spectral
266 bands were resampled to the 10 m pixel resolution bands. The 60 m pixel resolution bands (B1, B9,
267 B10) that support atmospheric correction, but are not optimal for land surface classification, were
268 removed. We added the normalized difference vegetation index (NDVI; NIR-RED / NIR + RED) to
269 the band collection.

Deleted: S-2

Deleted: S-2

270 3.4.3 Central delta habitat classification

271 Sentinel-2 pixels from the 30 x 30 m ESUs (dataset 1, Shevtsova et al. 2021a), and additional
272 polygons (Figure A3) defined by expert knowledge, led to 8 626 labelled pixels for the habitat
273 classification (labelled pixels are published in the Landgraf et al 2022a data collection). From those 8
274 626 pixels we randomly selected 50 % for the training and 50 % for validation. Polygons were
275 defined by BH, based on high resolution RGB satellite images, and in areas that have been visited
276 regularly during field expeditions. We tested several classifiers and different selected band
277 combinations (spectral bands and NDVI). Water (transparent to turbid) and sandbanks were omitted
278 in the classification processing by masking them as inactive using a band threshold; water mask was
279 based on the NIR 10 m band 8 (NIR < 0.02) and the sand mask was based on the blue 10 m band 2
280 (Blue > 0.07, Table 1). The classification was tuned to depict vegetation composition and was
281 qualitatively assessed well known to the classification developers. Best results for the habitat
282 classification were obtained using a random forest classification with a band combination of all

Deleted: S-2

Deleted:

Deleted: training pixels

Deleted: (50% to train the classifier and 50% for validation)...for the habitat classification for the habitat classification

Deleted: for the habitat classification

Deleted: training points

Deleted: shown in Appendix A4 and

295 [Sentinel-2](#) VIS, Red-Edge, NIR and SWIR bands, and the NDVI. The chosen classifier was able to
296 distinguish between relevant classes (Table 1) and could even identify patchy spots of specific
297 habitat classes. In addition to the defined water and sand classes, the final central Lena Delta
298 classification contains 10 habitat classes (Table 1). The here defined central Lena Delta covers an
299 area of 644.9 km² with a 55.2 % vegetation cover.

300 To assess the classification performance, we applied a cross-validation on an independent random
301 selection of the training pixels (50 %). Based on a confusion matrix (supplementary table S5), the
302 classification accuracy was 96.78 % ([class-based accuracy shown in Table A1](#)). However, this is
303 partly due to autocorrelation resulting from pixel selection within polygons. More importantly, the
304 accuracy was qualitatively tuned and evaluated based on ground-truthed knowledge of the
305 development team. The published dataset of Landgraf et al. (2022,
306 <https://doi.pangaea.de/10.1594/PANGAEA.945057>) provides the central Lena Delta habitat
307 classification map, the ESUs and the polygons used to train the classifier. The training dataset
308 includes data from 23 of the 26 vegetation plots (dataset 1). The dataset provides additional 69
309 ESUs defined with expert knowledge gathered during several field expeditions to the Lena Delta,
310 labeled as pseudo ESUs for potential future investigations.

311 3.5 Lena Delta habitat classification (Dataset 5)

312 3.5.1 Lena Delta habitat classes

313 In order to extend the habitat classification map to the entire Lena Delta (29873.7 km²), we included
314 all the habitat classes covering the central Lena Delta (dataset 4, table 1). In addition, and based on
315 expert knowledge as well as extensive visual satellite image investigations, we added one habitat
316 class that is not present in the central Lena Delta: the second terrace in the northwest of the Lena
317 Delta is lithologically and geomorphologically different from the other two terraces present in the
318 central delta, and characterized by sandy substrates. In a hyperspectral CHRIS PROBA satellite-
319 based geomorphological classification, Ulrich et al. (2009) described the second terrace featuring
320 very dry elevated sandbanks, barren or poorly vegetated areas with isolated lichens, moss, herbs,
321 dwarf shrubs or grasses (vegetation cover 0–60%, growth height: max. 20 cm, average active layer
322 depth of 1 m on the upland plain with old, vegetation-arrested sand dunes). Based on photos taken
323 at few locations in the field during past expeditions (see supplementary table S3) the habitat class
324 shows well-drained areas dominated by sandy substrate and diverse, sparse vegetation cover; some
325 areas are dominated by sedges, cotton grass and mosses with rare occurrences of lichens and
326 dwarf shrubs, while some areas are dominated by the latter. Schneider et al. (2009) defined the
327 same class as 'dry moss-, sedge- and dwarf shrub-dominated tundra (DMSD)'. We selected 35
328 ESUs for this habitat class characterized by high SWIR reflectance ([Sentinel-2](#) band 11) due to dry

Deleted: S-2

Deleted: S-2

331 land surface conditions. The habitat class was named 'dwarf shrub - herb communities' and was
332 added as an additional habitat class to the training data set.

333

334 3.5.2 Satellite data processing

335 The Lena Delta habitat classification was based on a Sentinel-2 mosaic (top of atmosphere (TOA)
336 reflectance, Google Earth Engine Dataset) with images taken of the area between June 1 and
337 September 15, 2018. The images (N = 1685, distributed across 15 Sentinel-2 tiles) were filtered to
338 discard images with cloud cover above 20%. A cloud mask was applied to the remaining 262
339 images, masking pixels where the quality band 'QA60' indicates clouds (band 10) or cirrus (band
340 11). All spectral bands with 20 m resolution were resampled to match the 10 m resolution bands.
341 Next, NDVI was computed (see 3.4) for each image and one high-quality mosaic of all images based
342 on the maximum NDVI value per pixel was produced representing a snapshot of the peak summer
343 vegetation period. Using the median NIR band values across the 262 cloud-masked images, we
344 classified water with a threshold of < 0.07 reflectance. The remaining non-vegetated areas defined
345 by a threshold of NDVI < 0.4 were classified as barren/sand. The water- and sand-masked image
346 mosaics were then used in the classification pipeline with the following bands: B2 (blue), B3 (green),
347 B4 (red), B5 (red edge 1), B6 (red edge 2), B7 (red edge 3), B8 (NIR), B11 (SWIR 1), B12 (SWIR 2),
348 and NDVI.

349 3.5.3 Lena Delta Habitat classification

350 From the central Lena Delta habitat classification (dataset 4) we sampled 7 500 random pixels to
351 train a random forest classifier (smileRandomForest in Google Earth Engine). In addition, we added
352 35 pixels from the ESUs selected within the 'dwarf shrub - herb communities' of the north-western
353 Lena Delta. Given the dominance of the 'dwarf shrub – herb communities' on the second terrace
354 (north-eastern part of the Lena Delta), the confidence of selecting correct training pixels for this
355 habitat was relative high (see also Figure S7). Unfortunately, no vegetation recording or monitoring
356 schemes exist outside the central Lena Delta. We thus lack format independent validation of the
357 classification across the Delta. Based on confusion matrix, the overall accuracy of the classifier
358 based on its training data (i.e., resubstitution error) was 96.47 %. Habitat class accuracy varied
359 between 91.89 % and 100 % (see complete confusion matrix in Table A2). Similar to the validation
360 of the central Lena Delta habitat classification, the results were carefully checked to make sure that
361 large-scale pattern, e.g., differences between the three terraces, are accurately separated, and that

Deleted: S-2

Deleted: S-2

Deleted: /

Deleted: Therefore, independent validation of the classification across the Delta is not possible.

Deleted: with expert knowledge from the central Delta and a few adjacent regions that are known to the developer team...

370 [the highly repetitive structures within terraces are also recognized by the classification \(see Figures](#)
371 [S6-S8\)](#).

372 Since the barren/sandy areas are highly dynamic with variable water levels mainly within (due to
373 flooding in spring and decreasing river flow during the summer season) but also across years
374 (discharge dynamics), we computed a sandbar probability map for the Lena Delta using cloud
375 masked [Sentinel-2](#) (TOA reflectance) images between April 1 and October 15 from 2015 to 2021 (6
376 026 images). In each image, we labeled sandy pixels by $NDVI < 0.4$ AND $NDWI > 0.095$ AND $NIR <$
377 0.09 reflectance. Next, for each pixel in the Lena Delta, we computed the percentage of sandy pixels
378 across all images resulting in a sand probability map. The training dataset (random 7500 points, plus
379 35 points with label 'dwarf shrubs - herb communities'), the habitat classification, and the sandbar
380 probability map was published in the PANGAEA repository (Figure 5, Lisovski et al., 2022,
381 <https://doi.pangaea.de/10.1594/PANGAEA.946407>).

382 3.6 Lena Delta disturbance regimes (Dataset 6)

383 The Lena Delta experiences different disturbance regimes, mapped and described in dataset 6.
384 Mainly annual flooding, but also local rapid thaw processes on the land surface of the terraces with
385 ice-rich permafrost, result in disturbance regimes forming distinct habitat classes (Table 2). The
386 floodplains experience seasonal flooding as a regularly occurring disturbance in spring after ice-
387 break up (the spring flood). Very high disturbance regimes due to the most intense scour, erosion
388 and sedimentation result in barren sandbanks or in early-stage plant communities equalling the
389 'sparsely vegetated' habitat class. The classes 'moist to wet sedge communities', 'wet sedge
390 communities', 'moist equisetum and shrubs', 'dry shrub communities', 'dry grass to wet sedge
391 communities' represent the mid to advanced successional stages on the floodplain within areas of
392 high disturbance that are also described as shifting habitat class (Stanford et al., 2005; Driscoll and
393 Hauer, 2019).

394 In contrast to the high disturbance regimes on the floodplain, habitats on the first, second and third
395 delta terraces are less extensively disturbed (low disturbance). In these areas typical mature-state
396 tundra plant communities are able to develop; 'polygonal tundra complex', 'tussock tundra', and
397 'dwarsh shrub herb communities'. However, locally, high disturbance occurs by rapid thaw
398 processes of ice-rich permafrost on the first and third delta terraces with habitats characterized by
399 mid to advanced-stage plant succession; 'moist to wet sedge communities', 'wet sedge
400 communities', 'dry shrub communities', and 'dry grass to wet sedge' communities. Very high
401 disturbance due to intense rapid thaw processes occurs at eroding cliffs and lake margins, in steep
402 valleys and actively developing gullies resulting in barren surfaces with rims of sparsely vegetated

Deleted: . Together with visual comparison of high resolution ESRI RGB satellite background images, we consider the results accurate. A formal validation based on another random sample of 5 000 points from the central Delta showed expected high accuracy of > 95 %.

Deleted: S-2

410 transition zones. Given the link between plant communities and flooding as well as rapid thaw
411 processes, we characterized the disturbance regimes for each habitat class (Table 2) and provide
412 mapped disturbance based on the habitat class of dataset 5 and the corresponding disturbance
413 regime for the entire Lena Delta (Figure 6, Heim and Lisovski, 2023,
414 <https://doi.org/10.5281/zenodo.7575691>).

415 4 Results and Discussion

416 We deliver a detailed description and associated data products of the most prominent habitat
417 classes in the largest Arctic river delta, the Lena Delta. Supported by ecological field data of plant
418 composition, hyperspectral field measurements from the same sites, and regional expert knowledge
419 collected over decades, we develop a high-resolution [Sentinel-2](#) based habitat map for the entire
420 delta. The compiled datasets provide the necessary baseline for future investigations of the
421 biochemical processes, ecological dynamics, and responses to global warming within the Arctic
422 tundra system of the delta.

423 4.1 Habitat classes of the Lena Delta

424 Based on the floristic composition and biomass of the vegetation plots (Dataset 1, 2), the spectral
425 properties from hyperspectral field measurements (Dataset 3) as well as expert knowledge, we
426 defined 11 distinct habitat classes linked to different vegetation composition for the Lena Delta
427 (Figure 4). The selected [Sentinel-2](#) spectral bands and the derived NDVI values allow a separation
428 of the habitat classes into two distinct groups (the first separation level between habitat classes in
429 Figure 4a, 1st hierarchical level). Three habitat classes ('wet sedge communities', 'moist Equisetum
430 and shrub communities', 'dry grass to wet sedge communities') formed in areas of high disturbance
431 by rapid thaw processes and regular flooding represent a distinct cluster with highest vegetation
432 vitality (high NDVI), and separated from the more stable and mature tundra communities ('polygonal
433 tundra complex', 'dry (tussock) tundra', and 'dry dwarf-shrub and herb communities'), and the other
434 successional plant communities ('moist to wet sedge complex', 'dry low shrub communities' and
435 'sparsely vegetated') all characterised by a lower NDVI range. The 'dry dwarf-shrub and herb
436 communities' form a separate cluster with the least overlap with other habitat classes within the two-
437 dimensional non-metric multidimensional scaling (NMDS) space (2nd hierarchical level, Figure 3a;
438 Figure 4c) due to very low vegetation vitality and surface moisture (lowest NDVI, high red and SWIR
439 reflectance). There are two remaining habitat classes on the 3rd and 4th hierarchical level, which are
440 successional plant communities, the 'moist to wet sedge complex' and 'dry low shrub communities'.
441 The separation on the 3rd and 4th hierarchical level is mainly driven by higher NDVI of these

Deleted: S-2

Deleted: S-2

444 successional plant community classes in comparison with the mature state tundra plant communities
445 with lower NDVI (Figure 4a-b). The 'dry grass to wet sedge communities' and the 'sparsely
446 vegetated area' habitat class (not covered by vegetation plots but added during the classification
447 process), show the largest overlap with the other habitat classes due to a high variability in
448 vegetation cover, biomass and moisture. In general, the ordination method (Figure 4b) shows that
449 distinct plant communities and the associated habitat classes are mostly separated by a biomass
450 gradient for which the NDVI is a good approximator. A further separation linked to potential spectral
451 proxies for biomass exists with the far red-edge and NIR bands (B6,7,8) but is less distinct than the
452 NDVI axis. Together with the SWIR (B11,12) the red (B4) and near red-edge (B5) bands, and less
453 strongly the blue and green bands (B2,3), the results indicate a habitat class separation based on
454 moisture, biomass and vegetation colour characteristics.

455 The vegetation plot selection was made in relation to the most typical habitats (e.g., Mueller-
456 Bombois and Ellenberg, 1974). For 15 of the 26 vegetation plots, we collected and provided
457 hyperspectral surface reflectance data (Runge et al., 2021). These measurements cover a variety of
458 landscape units including Yedoma uplands, floodplains (vegetated and non-vegetated), drained
459 thermokarst lake basins (old and recently drained), and areas covered by low shrub layers.

460 Comparing the hyperspectral surface reflectance with multispectral [Sentinel-2](#) data, we found
461 commonalities in the discrimination of habitat classes along moisture gradients. Unfortunately, the
462 hyperspectral field measurements do not cover the biomass gradient. Plot measurements with the
463 field spectrometer are conducted with the hand-held instrument held at shoulder height, hence it was
464 not possible to acquire field spectroscopy measurements in disturbed patches with tall shrubs or
465 very sloped terrain. This highlights the difficulty in deriving high spectral resolution surface
466 reflectance measurements representative of fine scale differences between Arctic tundra habitat
467 classes if the plot properties become too challenging to measure.

468 In general, mature-state tundra plant communities have relatively similar spectral properties due to
469 low vascular plant cover (e.g., Beamish et al., 2017). In addition, the tundra vegetation communities
470 contain a wide range of accessory pigment composition (carotenoids and anthocyanins) that result in
471 a very similar spectral response (Beamish et al., 2018). Only the highly disturbed communities such
472 as wetlands or areas with tall shrubs are more spectrally distinct due to a high NIR reflectance
473 plateau (Buchhorn et al., 2013). Since the hyperspectral field measurements provide a higher spatial
474 resolution and thus also a measure of variability within areas of the same general habitat type, we
475 consider the measurements valuable for applications that aim at analysing ecological and
476 biochemical processes within distinct habitats in more detail.

477 **4.2 Sentinel-2 based habitat classification**

Deleted: S-2

479 Based on the identified habitat classes (Table 1) we applied a random forest classifier to map habitat
480 classes in the central Lena Delta and subsequently in the entire Lena Delta. Both maps represent
481 the summer season of 2018 for which we could use a sufficient number of satellite images with low
482 cloud cover.

483 The Lena Delta habitat map shows the ice-rich first and third terraces mainly covered by i) the
484 'polygonal tundra complex' due to impeded drainage on the terrace plateaus and by ii) drier tundra
485 communities on well drained areas due to older degraded permafrost forms (detailed description in
486 Morgenstern et al., 2008, 2011). On the second terrace, the classified 'dry dwarf shrub and herb
487 communities' occur well separated from the moist habitat classes covering the floor of the alases.
488 On the floodplains, the rich mosaic outlines a wide spectrum of very diverse classes, the dry versus
489 moist and wet substrate habitats, in the active delta area.

490 Polygonal tundra is characterized by high spatial heterogeneity; at the decimeter to meter-scale
491 plant composition and diversity is defined by the polygonal microrelief and water level (Whitaker and
492 Woodwell, 1968; Forman and Godron, 1981; Zibulski et al., 2016; Nitzbon et al., 2020, Siewert et al.,
493 2021). Therefore, within a single Sentinel-2 pixel, dry polygonal rims, moist slopes, wet patches and
494 surface water can all be present. The spatial resolution of Sentinel-2 cannot capture the meter-scale,
495 but captures the heterogeneity between the different surface water contributions of the 'polygonal
496 tundra complex' on the first and third terrace. In the Lena Delta, the 'polygonal tundra complex with
497 up to 50% surface water' represents the dominant habitat class with 25% of the delta area (about 7
498 434 km²). All other habitat classes represent 1-6% of the delta area with 'dwarf shrub-herb
499 communities' and 'moist to wet sedge complex' reaching 5.4% and 5.9%, respectively (Figure 6).

500 Based on the summer Sentinel-2 mosaic, the classes 'Water' and 'Sand' cover more than 40% of the
501 delta. However, those two classes are extremely variable within and across years, depending on the
502 river water level during image acquisition time. To provide information on this variability, we
503 calculated how often each pixel in the delta (cloud free Sentinel-2 pixels from 2015 to 2022) was
504 classified as sand (threshold approach). This led to an additional sand probability layer with values
505 between 0-100%.

506 Despite extensive research within the area, only a few classification products are available for the
507 Lena Delta. The new Lena Delta classification is a high-resolution (Sentinel-2, 10 m) map that
508 focuses on the delta-specific habitat classes and emphasizes the high level of heterogeneity across
509 the delta. We compared the Lena Delta habitat classification to existing classifications: the first
510 published Lena Delta-wide land cover classification targeted towards tundra environments and the
511 upscaling of methane emissions with 30 m resolution (Schneider et al., 2009), the global ESA
512 Climate Change Initiative CCI land cover classification with 300 m resolution (Defourny, 2019), and a

Deleted: S-2

Deleted: S-2

Deleted: S-2

Deleted: S-2

Deleted: S-2

518 circum-arctic standardized ESA GlobPermafrost land cover map of the Lena Delta with 20 m
519 resolution (Bartsch et al., 2019). We sampled the classification results with a regular point grid of
520 more than 3 million points which have an equal distance of 100 m to one another to compare the
521 classification results. Figures and tables with more information on class comparisons can be found in
522 the supplements (Table 1, Figure S3, S4m, S5). Overall, the classifications of the Lena Delta overlap
523 well for 'water' (water bodies (Defourny, 2019), shallow water (Schneider et al., 2009), water
524 (different depths and sediment yields, Bartsch et al. 2019)) and 'sand' (bare areas (Defourny, 2019),
525 mainly non-vegetated areas (Schneider et al., 2009), sand, seasonally inundated and disturbed
526 (Bartsch et al. 2019)) areas. Besides this, the mapped classes differ greatly from one another. For
527 example, the dominant classes in the coarse ESA CCI land cover 2018 product (300 m) for the Lena
528 Delta are 'shrub or herbaceous cover', 'flooded', 'fresh / saline / brackish water', 'sparse vegetation
529 (tree, shrub, herbaceous cover) (<15%)', and 'mosaic tree and shrub (>50%)', 'herbaceous cover
530 (>50%)'.

531 These broad classes describe the major land cover in the Arctic delta but fail to depict the
532 heterogeneity of habitats and plant communities not only because of its coarse spatial resolution but
533 also because of the broad class descriptions. Furthermore, smaller areas are classified as 'tree
534 cover', 'needleleaved', 'evergreen / deciduous', 'closed to open (>15%)' and 'mosaic tree and shrub
535 (>50%) / herbaceous cover (<50%)' which is an inaccurate depiction of the delta.

536 This habitat map and the land cover classification from Schneider et al. (2009) resemble each other
537 more closely, however, this habitat map shows more differentiation in the classes and spatial
538 resolution, 10 m to 30 m, respectively. The only class description that is identical in both
539 classifications, besides water and sand / mainly non-vegetated areas, is 'dry tussock tundra'.
540 However, there is only a small match between these classes in the point comparison and most 'dry
541 tussock tundra' areas from the Schneider et al. (2009) classification fall into the PC_50%, PC_20%,
542 'moist wet sedge complex' and 'dwarf shrub-herb communities'. The habitat map shows the mosaic
543 of habitats on the floodplain with 'moist equisetum and shrubs on floodplain', 'dry low shrub
544 community', 'moist to wet sedge' and 'wet sedge complex' which match with 'moist to dry dwarf
545 shrub-dominated tundra' in the land cover classification of Schneider et al. (2009). Also, for the
546 polygonal tundra complex, our habitat map shows more differentiation with three classes of up to
547 50% 20% 10% surface water contribution versus two classes in Schneider et al. (2009) 'wet sedge
548 and moss dominated tundra' and 'moist grass and moss dominated tundra' The areas covered by
549 'PC_50%' and 'PC_20%' match with 'wet sedge- and moss-dominated tundra', and 'PC_20%' and
550 'PC_10%' match with 'moist grass and moss-dominated tundra'. The overall aim of both maps is to
551 differentiate between dry to wet land cover habitats as these describe the heterogeneity in the delta

552 well and determine factors related to methane emissions (see Schneider et al. 2009) and the
553 different habitat classes.

554 The land cover classification from ESA GlobPermafrost differentiates between 21 classes which are
555 associated to eight broader groups, such as sparse vegetation, shrub tundra, forest, grassland,
556 floodplain, disturbed, barren and water (Bartsch et al., 2019). With a spatial resolution of 20 m, the
557 latter product is the closest to this habitat map. The major class 'wet ecotopes' of ESA
558 GlobPermafrost match with our 'PC_50%:' on the first terrace and the 'moist to wet sedge complex'
559 on the floodplains. On the floodplain however, other classes show less agreement. The ESA
560 GlobPermafrost one class 'floodplain mostly fluvial' does not differentiate the floodplain classes
561 further, in contrast to our habitat map differentiating between 'moist to wet sedge complex', 'wet
562 sedge complex', 'moist equisetum and shrubs' and 'dry low shrub community' on floodplain.
563 Whereas the ESA GlobPermafrost class 'disturbed' (defined as forest fire scars, seasonally
564 inundation and landslide scars can be found in 'PC_50%' predominantly, in 'sand', 'PC_20%' and
565 'sparsely vegetated areas' in our habitat map. This underlines the complex structure of match and
566 mismatch between classifications.

567 The land cover map from Schneider et al. (2009) is based on two cloud-free Landsat images from
568 June/July 2000 and 2001, the ESA CCI land cover 2018 map is based on summer images as well.
569 Hence, the images used for this habitat classification were acquired at a similar time as for the ESA
570 CCI product and we do not expect differences based on changes on the ground due to this temporal
571 concurrence. In the almost 20-year difference between Schneider et al. (2009) and this habitat map
572 we do expect changes in vegetation composition. Overall, it is challenging to obtain sufficient cloud-
573 free images during the summer months to fully cover the entire Lena Delta for a classification project
574 and to depict a specific phenological state. Therefore, we created a Sentinel-2 composite mosaic
575 based on the maximum NDVI value per pixel from June to September. With this we ensure to have
576 the peak vegetation and phenology season represented as input for the habitat classification as
577 much as possible and increase comparability to other classification studies despite a temporal
578 mismatch.

579 The habitat map gives an accurate and detailed description of the Arctic Lena Delta that
580 incorporates extensive field data and expert knowledge. The habitat map is superior to the ESA CCI
581 land cover map (2018) in both spatial resolution and class description as it depicts the
582 heterogeneous habitat distribution. The 20m ESA GlobPermafrost classification matches the
583 resolution of the habitat map closely but due to its wider geographical application with circum-Arctic
584 standardized classes it does not optimally represent Lena Delta-specific habitats, such as the widely
585 distributed polygonal tundra complex. Furthermore, the habitat map is an update to Schneider et al.

586 (2009), which was based on three Landsat images from 2000 and 2001 and shows further
587 differentiation of habitats, specifically representing the floodplain mosaics of this Arctic delta. [Note,](#)
588 [that the lack of independent validation plots/pixels across the Lena Delta limits our ability to formally](#)
589 [assess overall accuracy. This limitation might especially affect the smaller patchy habitat types,](#)
590 [rather than the dominant types within the three terraces \(see also visual evaluation in Figures S6-](#)
591 [S8\).](#)

592 **4.3 Habitat linked disturbance regimes**

593 Parts of the Lena Delta are characterised by disturbances due to annual floodings or rapid
594 permafrost thaw processes leading to specific habitat classes. We provide habitat linked disturbance
595 regimes (describing the type and intensity of disturbances) across the delta. Our product (Dataset 6,
596 Figure 6a) shows that the largest part of the vegetated delta (excluding 12 439 km² of 'sand' and
597 'water' classes) is impacted by low disturbance, resulting in mature-state plant communities on the
598 terrace plateaus (Figure 6b, 72%, 12 806 km²). Specifically, the second terrace in the northwest of
599 the delta, with low ice content, is least impacted by rapid thaw processes and not part of the active
600 delta. In contrast, the habitats in the active delta are all linked to high disturbance (27%, 4 875 km²).
601 The 'moist to wet sedge complex' (10% of the vegetated Lena Delta) is the largest class considered
602 to be formed by high disturbance. This class is found in larger patch sizes on the riverine floodplains,
603 smaller patches on the floor of thermo-erosional valleys. Overall, 27.5% of the vegetated area of the
604 Lena Delta experiences some level of high disturbance from either regular spring floods or from
605 rapid thaw processes.

606 Species richness, relative abundance and biomass characteristics are important habitat features that
607 are influenced by landscape characteristics such as topography, water fluxes, soil types and
608 disturbance regimes (Forman and Godron, 1981; Naiman et al., 1986; Pickett et al., 1989;
609 Montgomery, 1999). Greig-Smith (1964), Woodwell and Whittaker (1968), and Forman and Godron
610 (1981) described fragmentation of land surfaces due to disturbance (defined by type and intensities)
611 and topography. In the Lena Delta, the terrace-related topography and active floodplain areas are
612 major determinants of plant communities and habitat classes and are thus well reflected in the Lena
613 Delta habitat map.

614 The high disturbance regime on floodplains results in 'shifting habitats' (Stanford et al., 2005; Driscoll
615 and Hauer, 2019). The annual spring floods and rapid thaw processes result in areas of high
616 disturbances, habitats of mid to advanced plant successional stages showing high vascular plant
617 above ground biomass (Figure 6c) due to the higher nutrient availability, a deeper active layer and
618 more moisture (e.g., Myers-Smith et al., 2020). Within the low disturbance habitat classes, a thick

619 moss layer as well as a low vascular plant coverage characterise the tundra community
620 assemblages representing mature state plant communities. Because high disturbance patches are
621 characterized by high vascular biomass, they can be well classified specifically in the NDVI, but also
622 NIR and red edge bands of optical medium resolution sensors such as SENTINEL-2. Within the
623 vegetation plots (Dataset 1), we did not find clear differences in species richness and in the Shannon
624 diversity index between the disturbed and the undisturbed classes (Figure 6d). Since most disturbed
625 habitat classes such as the 'moist to wet sedge', the 'wet sedge' as well as homogeneous patches of
626 high shrubs (as part of the habitat class 'dry grass to wet sedge complex'), were not sampled in the
627 field due to too challenging conditions, however they are clearly representing habitats with low
628 species richness. In the extreme case disturbance can lead to barren and sparsely vegetated
629 surfaces.

Deleted: S-2

630 **4.4 Classification accuracy and representativeness**

631 The field data was acquired during a field trip in July-August 2018, primarily focusing on 30 m x 30 m
632 homogeneous vegetation and land cover plots. Additionally, we relied on Sentinel-2 images for the
633 different classifications that were also acquired in summer 2018, covering the same period as the
634 field trip, and have a spatial resolution of 20 m. The temporal overlap of the field work and the
635 satellite image acquisitions ensures consistency across the different datasets and represents a close
636 relationship between datasets and products obtained in the field (dataset 1, 2 and 3) and the results
637 derived from the satellite images that use the field data as input. As Sentinel-2 images have a small
638 geolocation error, we could link our field plot locations directly with the satellite images. Furthermore,
639 the sampling and measurement design of the plots with 30 m x 30 m ensured a reliable link to the
640 satellite data with similar spatial resolution, as we followed the recommendations on ESU. The
641 RGBNIR Sentinel-2 bands have a spatial resolution of 10 m and the red edge (NIR) and SWIR
642 bands a spatial resolution of 20 m, and even if we downsampled the bands to 10 m the spectral
643 information is sustained. More information on datasets and their spatial and temporal resolutions are
644 provided in supplementary Table S3.

645 The presented datasets are limited by the regional in-situ observations and expert knowledge
646 collected mainly in the central Lena Delta. The remoteness of the area and extremely difficult
647 logistics to conduct research in the second terrace and the outer rims of the delta are major reasons
648 for these limitations. However, the delta is relatively homogeneous in habitat classes that develop
649 based on underlying geomorphology and the disturbance regime (annual flooding and permafrost
650 thaw processes). Only one major habitat class is absent from the well studied central Lena Delta and
651 only occurs across the second terrace. Thus, even though detailed knowledge and in-situ
652 observations are derived from a relatively small subset of the Delta, we are confident that our

654 mapping results from the entire region are valuable and accurate. Also due to the inaccessibility of
655 large areas of the delta, quantitative accuracy assessments of the classifier and the final mapping
656 product are lacking. We had to rely on qualitative evaluation procedures by experts. Analysis of
657 similarity of habitat classes and SENTINEL-2 spectral reflectance as well as NDVI values provide
658 additional quantitative and qualitative assessments on the extent to which the different classes are
659 identifiable and separated between classes.

Deleted: S-2

660 In-situ observations (Datasets 1-3) as well as mapping products (Datasets 4-6) represent conditions
661 and vegetation composition of 2018. The timing of the summer 2018 expedition coincided with a
662 relatively high number of cloud free Sentinel-2 images necessary for a high quality habitat
663 classification. Overall, the described datasets are of appropriate quality to serve as a basis for
664 additional studies and most importantly as a baseline to identify changes in the future.

Deleted: S-2

665 5 Conclusions

666 The described datasets provide coherent and complementary information of the major habitat
667 classes in the Lena Delta in Arctic Siberia, the largest delta in the Arctic. Based on extensive
668 knowledge collected during fieldwork that included habitat-related measurements of plant
669 composition, biomass, and hyperspectral field measurements we provide a validated and high-
670 resolution habitat classification map of the delta. In addition, we linked ecologically important
671 characteristics of disturbances in the delta to habitat classes, providing a baseline for future studies
672 of Arctic change as well as a foundation for potential upscaling of related processes such as
673 biodiversity, ecosystem functions, and biochemical dynamics such as greenhouse gas emissions.
674 With this update of previous land cover and habitat-related mapping products of the Lena Delta we
675 strive to facilitate and promote future investigations leading to a better understanding of this highly
676 sensitive arctic delta system.

677 Acknowledgements

678 Field work in the Lena River Delta was conducted in the frame of the Russian-German LENA
679 Expeditions based at Research Station Samoylov Island. We thank all colleagues and station staff
680 involved in the organization and logistics for their great support.

683 Code/Data availability

- 684 Dataset 1: Shevtsova et al., 2021a, <https://doi.pangaea.de/10.1594/PANGAEA.935875>, Foliage
685 projective cover of 26 vegetation sites in the central Lena Delta from 2018, is published as Foliage
686 projective cover for all major taxa estimated as percent, as tab-delimited text files.
- 687 Dataset 2: Shevtsova et al., 2021b, <https://doi.pangaea.de/10.1594/PANGAEA.935923>, Total above-
688 ground biomass of 25 vegetation sites in the central Lena Delta from 2018, is published as biomass
689 aboveground dry mass per major taxa, as well as for 'moss and lichen', 'litter' and the remaining minor
690 taxa (called 'other plants') and the total biomass in the units [g/m²], as tab-delimited text.
- 691 Dataset 3: Runge et al., 2022, <https://doi.pangaea.de/10.1594/PANGAEA.945982>, Hyperspectral field
692 spectrometry of Arctic vegetation units in the central Lena Delta, is published as an overview of the
693 plot details and field spectrometer reflectance spectra in the unit [%] of 28 vegetation plots, as tab-
694 delimited text files.
- 695 Dataset 4: Landgraf et al., 2022 a,b,c. The Sentinel-2-derived central Lena Delta land cover (habitat)
696 classification consists of the following three data publications: i) Landgraf et al. 2022a,
697 <https://doi.pangaea.de/10.1594/PANGAEA.945056>: a raster file with assigned land cover classes and an
698 ESRI polygon shape file containing the 10 training classes representing the different vegetation
699 compositions, as geotiff file. Both datasets are based on 2018 satellite images and informed by the in-
700 situ vegetation plots and expert knowledge. Datasets are in Universe Transverse Mercator (UTM) Zone
701 52 North projection. ii) Landgraf et al. 2022b, <https://doi.pangaea.de/10.1594/PANGAEA.945054>. This
702 data set includes training elements representing different vegetation composition in the form of
703 Elementary Sampling Units ESUs: 69 pseudo ESUs set with expert knowledge from the field and from
704 Lena Delta expedition field reports. iii) Landgraf et al. 2022c,
705 <https://doi.pangaea.de/10.1594/PANGAEA.945055>. This data set includes training elements representing
706 different vegetation composition in the form of Elementary Sampling Units ESUs: 23 true ESUs
707 representing the LD18 vegetation plots.
- 708 Dataset 5: Lisovski et al., 2022, <https://doi.pangaea.de/10.1594/PANGAEA.946407>. The Lena Delta
709 Habitat Map (2018, Sentinel-2) contains i) the Lena Delta habitat map (13 classes), ii) the sand probability
710 map, both as geotiff files in WGS84 geographic projection, iii) the habitat class description as comma
711 delimited csv table, and iv) the training dataset (n = 4 278 classified pixels) in geographic decimal
712 coordinates comma delimited csv table. The data collection also contains the Lena Delta Region of
713 Interest (ROI) ESRI shapefile outlining the Lena Delta including a coastal water buffer.

714 Dataset 6: Heim and Lisovski, 2023, <https://doi.org/10.5281/zenodo.7575691>. The Lena Delta habitat
715 disturbance regime map is published in the form of two geotiff files (tiles) in WGS84 geographic
716 projection.

717 Code developed in Google Earth Engine to derive habitat classes based in the central Lena Delta
718 classification, as well as R code for figures can be accessed from the following repository: Lisovski,
719 S. (2024). Code for 'A new habitat map of the Lena Delta in Arctic Siberia based on field and remote
720 sensing datasets'. V0.1. Zenodo. 10.5281/zenodo.11197641.

721 Competing interests

722 Birgit Heim is a member of the editorial board of ESSD. Otherwise, we declare no competing interests.

723 Funding

724 SL acknowledges funding from the Geo.X Network for Geosciences in Berlin and Brandenburg. This
725 study was supported by BMBF KoPf (Grant Number 03F0764B), KoPf Synthesis (Grant Number
726 03F0834B), and AWI base funds. AR was partially funded by ESA GlobPermafrost and an ESA CCI
727 postdoctoral fellowship. BH acknowledges HGF REKLIM.

728 Authors contribution

729 SL: Conceptual framework, habitat classification, data analysis, writing

730 AR: Conceptual framework, field work, spectral field data collection, habitat classification, spectral
731 data processing, data analysis, writing

732 IS: Field work, biomass and projective cover measurement in vegetation plots, habitat classification

733 RRO: Habitat classification

734 NL: habitat classification, spectral data processing

735 MF: Field work, spectral field data collection

736 NiL: habitat class definition, field work

737 AM: Project management, writing

738 CS: Spectral data processing

739 AB: Spectral data processing

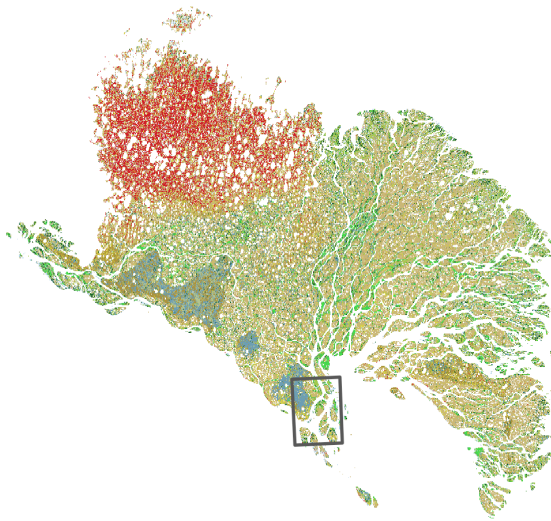
740 UH: Conceptual framework, project management

741 GG: Conceptual framework, project management, habitat classification, writing

742 BH: Conceptual framework, field work, habitat classification, project management, writing

743 Appendix

Deleted:Page Break.....
↑



744
745 *Figure A1: Location of the central Lena Delta (Dataset 4) in the Lena Delta (Dataset 5,6). WGS 84 projection.*
746

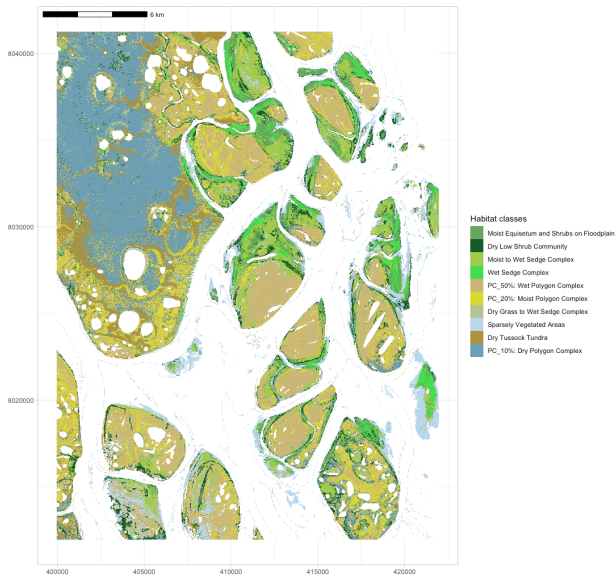


Figure A2: Supervised habitat classification of the central Lena Delta based on a cloud-free *Sentinel-2* August 2018 acquisition (Dataset 4). Numbers in legend correspond to the labels in published Dataset 4 (Landgraf et al. 2022). Universe Transverse Mercator Z52 on WGS 84 projection.

Deleted: S-2

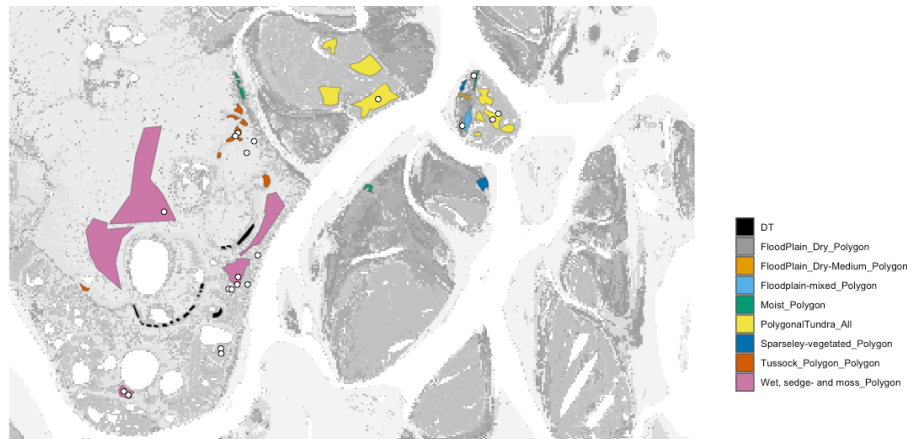


Figure A3: Subset of the central Lena Delta with 30 x 30 m ESUs (white points, dataset 1) and polygons defined by expert knowledge (published with dataset 4). Together the ESUs and polygons served areas to sample 8 626 training pixels for the central Lena Delta landcover/habitat classification (dataset 4, Landgraf et al. 2022a).

Table A1: Results of the class-based cross-validation for the central Lena Delta habitat classification, based in 50 % of the 8 626 labelled pixels, and the accuracy of the classifier (e.g., resubstitution error) of the entire Lena Delta habitat classifier.

Deleted: ¶

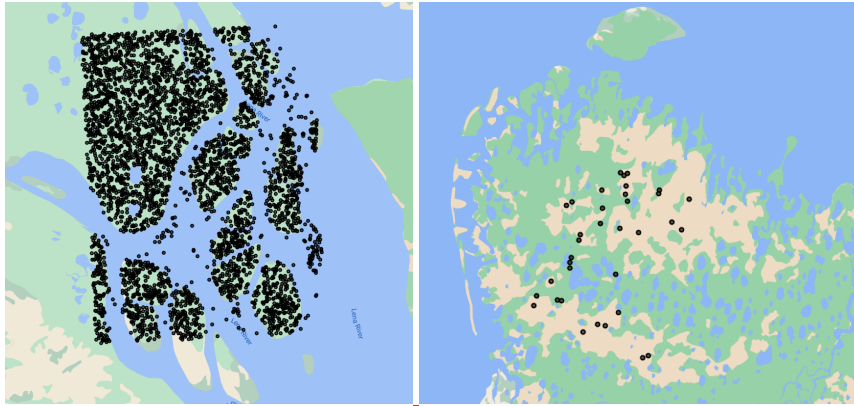
Formatted: Not Highlight

Habitat class	Abbreviation	Accuracy – central Lena Delta	Accuracy – entire Lena Delta
Moist equisetum and shrub community	MESH	0.999	0.977
Dry shrub community	DSH	0.998	0.947
Moist to wet sedge community	MSWS	0.997	0.972
Wet sedge community	WS	0.991	0.947
Polygonal tundra (up to 50% surface water)	PC < 50%	0.988	0.978
Polygonal tundra (up to 20% surface water)	PC < 20%	0.986	0.925
Dry grass to wet sedge community	GSSH	0.990	0.918
Sparsely vegetated area	SPSH	0.999	0.948
Dry tundra (tussock tundra)	DT	0.993	0.94
Polygonal tundra (up to 10% surface water)	PC < 10%	0.996	0.985
Dwarf shrub-herb community	DSC	-	0.999

Formatted: Not Highlight

783

Deleted: ¶
¶



784

785

786 **Figure A4:** Training pixels for the Lena Delta habitat classification (dataset 5). (Left) 7,500 random pixels samples

787 across the habitat classes from the central Lena Delta landcover/habitat map (dataset 4). (Right) 35 pixels selected

788 by expert knowledge for the 'dwarf shrub - herb communities' that are missing in the central Lena Delta.

791 **References**

792 AMAP: AMAP Arctic Climate Change Update 2021: Key Trends and Impacts. Arctic Monitoring
793 and Assessment Programme (AMAP), Tromsø, Norway, viii+148pp, 2021.

794 Bartlett, K. B., Crill, P. M., Sass, R. L., Harriss, R. C., and Dise, N. B.: Methane Emissions from
795 Tundra Environments in the Yukon-Kuskokwim Delta, Alaska, *Journal of Geophysical*
796 *Research-Atmospheres*, 97, 16645-16660, doi: 10.1029/91jd00610, 1992.

797 Bartsch, A., Hofler, A., Kroisleitner, C., and Trofaier, A. M.: Land Cover Mapping in Northern
798 High Latitude Permafrost Regions with Satellite Data: Achievements and Remaining
799 Challenges, *Remote Sensing*, 8, 979. doi: 10.3390/rs8120979, 2016.

800 Bartsch, A., Widhalm, B., Pointner, G., Ermokhina, K., Leibman, M., and Heim, B.: Landcover
801 derived from Sentinel-1 and Sentinel-2 satellite data (2015-2018) for subarctic and arctic
802 environments [dataset], <https://doi.org/10.1594/PANGAEA.897916>, 2019.

803 Bartsch, A., Widhalm, B., Leibman, M., Ermokhina, K., Kumpula, T., Skarin, A., Wilcox, E. J.,
804 Jones, B. M., Frost, G. V., Hofler, A., and Pointner, G.: Feasibility of tundra vegetation height
805 retrieval from Sentinel-1 and Sentinel-2 data, *Remote Sensing of Environment*, 237, 111515,
806 doi: 10.1016/j.rse.2019.111515, 2020.

807 Beamish, A., Raynolds, M. K., Epstein, H., Frost, G. V., Macander, M. J., Bergstedt, H., Bartsch,
808 A., Kruse, S., Miles, V., Tanis, C. M., Heim, B., Fuchs, M., Chabrillat, S., Shevtsova, I.,
809 Verdonen, M., and Wagner, J.: Recent trends and remaining challenges for optical remote
810 sensing of Arctic tundra vegetation: A review and outlook, *Remote Sensing of Environment*,
811 246, ARTN 111872, doi: 10.1016/j.rse.2020.111872, 2020.

812 Beamish, A. L., Coops, N., Chabrillat, S., and Heim, B.: A Phenological Approach to Spectral
813 Differentiation of Low-Arctic Tundra Vegetation Communities, North Slope, Alaska, *Remote*
814 *Sensing*, 9, 1200, doi: 10.3390/rs9111200, 2017.

815 Beamish, A. L., Coops, N. C., Hermosilla, T., Chabrillat, S., and Heim, B.: Monitoring pigment-
816 driven vegetation changes in a low-Arctic tundra ecosystem using digital cameras, *Ecosphere*,
817 9, e02123, doi: 10.1002/ecs2.2123, 2018.

818 Berner, L. T., Massey, R., Jantz, P., Forbes, B. C., Macias-Fauria, M., Myers-Smith, I.,
819 Kumpula, T., Gauthier, G., Andreu-Hayles, L., Gaglioti, B. V., Burns, P., Zetterberg, P., D'Arrigo,
820 R., and Goetz, S. J.: Summer warming explains widespread but not uniform greening in the
821 Arctic tundra biome, *Nature Communications*, 11, 4621, doi: 10.1038/s41467-020-18479-5,
822 2020.

823 Biskaborn, B. K., Smith, S. L., Noetzli, J., Matthes, H., Vieira, G., Streletskiy, D. A., Schoeneich,
824 P., Romanovsky, V. E., Lewkowicz, A. G., Abramov, A., Allard, M., Boike, J., Cable, W. L.,
825 Christiansen, H. H., Delaloye, R., Diekmann, B., Drozdov, D., Etzelmuller, B., Grosse, G.,
826 Guglielmin, M., Ingeman-Nielsen, T., Isaksen, K., Ishikawa, M., Johannsson, M., Johannsson, H.,
827 Joo, A., Kaverin, D., Kholodov, A., Konstantinov, P., Kroger, T., Lambiel, C., Lanckman, J. P.,
828 Luo, D. L., Malkova, G., Meiklejohn, I., Moskalenko, N., Oliva, M., Phillips, M., Ramos, M.,
829 Sannel, A. B. K., Sergeev, D., Seybold, C., Skryabin, P., Vasiliev, A., Wu, Q. B., Yoshikawa, K.,
830 Zheleznyak, M., and Lantuit, H.: Permafrost is warming at a global scale, *Nature*
831 *Communications*, 10, 264, doi: 10.1038/s41467-018-08240-4, 2019.

832 Boike, J., Wille, C., and Abnizova, A.: Climatology and summer energy and water balance of
833 polygonal tundra in the Lena River Delta, Siberia, *Journal of Geophysical Research-*
834 *Biogeosciences*, 113, G03025, doi: 10.1029/2007jg000540, 2008.

835 Boike, J., Nitzbon, J., Anders, K., Grigoriev, M., Bolshiyarov, D., Langer, M., Lange, S.,
836 Bornemann, N., Morgenstern, A., Schreiber, P., Wille, C., Chadburn, S., Gouttevin, I., Burke, E.,
837 and Kutzbach, L.: A 16-year record (2002-2017) of permafrost, active-layer, and meteorological
838 conditions at the Samoylov Island Arctic permafrost research site, Lena River delta, northern
839 Siberia: an opportunity to validate remote-sensing data and land surface, snow, and permafrost
840 models, *Earth System Science Data*, 11, 261-299, doi: 10.5194/essd-11-261-2019, 2019.

841 Box, J. E., Colgan, W. T., Christensen, T. R., Schmidt, N. M., Lund, M., Parmentier, F. J. W.,
842 Brown, R., Bhatt, U. S., Euskirchen, E. S., Romanovsky, V. E., Walsh, J. E., Overland, J. E.,
843 Wang, M. Y., Corell, R. W., Meier, W. N., Wouters, B., Mernild, S., Mard, J., Pawlak, J., and
844 Olsen, M. S.: Key indicators of Arctic climate change: 1971-2017, *Environmental Research*
845 *Letters*, 14, 045010, doi: 10.1088/1748-9326/aafc1b, 2019.

846 Buchhorn, M., Walker, D. A., Heim, B., Reynolds, M. K., Epstein, H. E., and Schwieder, M.:
847 Ground-Based Hyperspectral Characterization of Alaska Tundra Vegetation along
848 Environmental Gradients, *Remote Sensing*, 5, 3971-4005, doi: 10.3390/rs5083971, 2013.

849 Driscoll, K. P. and Hauer, F. R.: Seasonal flooding affects habitat and landscape dynamics of a
850 gravel-bed river floodplain, *Freshwater Science*, 38, 510-526, doi: 10.1086/704826, 2019.

851 Drusch, M., Del Bello, U., Carlier, S., Colin, O., Fernandez, V., Gascon, F., Hoersch, B., Isola,
852 C., Laberinti, P., Martimort, P., Meygret, A., Spoto, F., Sy, O., Marchese, F., Bargellini, P.,
853 Sentinel-2: ESA's optical high-resolution mission for GMES operational services. *Rem. Sens.*
854 *Environ.*, 120, 25–36, doi: 10.1016/j.rse.2011.11.026 , 2012.

855 Duncanson, L., Armston, J., Disney, M., Avitabile, V., Barbier, N., Calders, K., Carter, S.,
856 Chave, J., Herold, M., MacBean, N., McRoberts, R., Minor, D., Paul, K., Réjou-Méchain, M.,
857 Roxburgh, S., Williams, M., Albinet, C., Baker, T., Bartholomeus, H., Bastin, J. F., Coomes, D.,
858 Crowther, T., Davies, S., de Bruin, S., De Kauwe, M., Domke, G., Dubayah, R., Falkowski, M.,
859 Fatoyinbo, L., Goetz, S., Jantz, P., Jonckheere, I., Jucker, T., Kay, H., Kellner, J., Labriere, N.,
860 Lucas, R., Mitchard, E., Morsdorf, F., Næsset, E., Park, T., Phillips, O. L., Ploton, P., Puliti, S.,
861 Quegan, S., Saatchi, S., Schaaf, C., Schepaschenko, D., Scipal, K., Stovall, A., Thiel, C.,
862 Wulder, M. A., Camacho, F., Nickeson, J., Román, M., and Margolis, H.: Aboveground Woody
863 Biomass Product Validation Good Practices Protocol. Version 1.0, Land Product Validation
864 Subgroup (WGCV/CEOS), doi:10.5067/doc/ceoswgcv/lpv/agb.001, 2021.

865 Endsley, K. A., Kimball, J. S., and Reichle, R. H.: Soil Respiration Phenology Improves Modeled
866 Phase of Terrestrial net Ecosystem Exchange in Northern Hemisphere, *Journal of Advances in*
867 *Modeling Earth Systems*, 14, e2021MS002804, doi: 10.1029/2021MS002804, 2022.

868 ESA, 2015. Sentinel-2 User Handbook. ESA Standard Document.

869 ESA Land Cover CCI project team; Defourny, P. (2019): ESA Land Cover Climate Change
870 Initiative (Land_Cover_cci): Global Land Cover Maps, Version 2.0.7. Centre for
871 Environmental Data Analysis, *downloaded 2022*, [dataset]
872 <https://catalogue.ceda.ac.uk/uuid/b382ebe6679d44b8b0e68ea4ef4b701c>

873 Fedorova, I., Chetverova, A., Bolshiyarov, D., Makarov, A., Boike, J., Heim, B., Morgenstern,
874 A., Overduin, P. P., Wegner, C., Kashina, V., Eulenburg, A., Dobrotina, E., and Sidorina, I.:
875 Lena Delta hydrology and geochemistry: long-term hydrological data and recent field
876 observations, *Biogeosciences*, 12, 345-363, doi: 10.5194/bg-12-345-2015, 2015.

877 Forman, R. T. T. and Godron, M.: Patches and Structural Components for a Landscape
878 Ecology, Bioscience, 31, 733-740, doi 10.2307/1308780, 1981.

879 Frost, G. V., Loehman, R. A., Saperstein, L. B., Macander, M. J., Nelson, P. R., Paradis, D. P.,
880 and Natali, S. M.: Multi-decadal patterns of vegetation succession after tundra fire on the
881 Yukon-Kuskokwim Delta, Alaska, Environmental Research Letters, 15, 025003, doi:
882 10.1088/1748-9326/ab5f49, 2020.

883 Gilg, O., Sané, R., Solovieva, D. V., Pozdnyakov, V. I., Sabard, B., Tsanos, D., Zöckler, C.,
884 Lappo, E. G., Syroechkovski, J. E. E., and Eichhorn, G.: Birds and Mammals of the Lena Delta
885 Nature Reserve, Siberia, ARCTIC, 53, 118-133, doi: 10.14430/arctic842, 2000.

886 Greig-Smith, P.: Quantitative plant ecology, Butterworths1964.

887 Grigoriev, M. N.: Crio Morphogenesis in the Lena Delta, Permafrost Institute Press, Yakutsk
888 1993.

889 Heim, B. and Lisovski, S.: Lena Delta habitat disturbance regimes (0.0) [dataset], Zenodo,
890 <https://doi.org/10.5281/zenodo,7575691>, 2023.

891 Holl, D., Wille, C., Sachs, T., Schreiber, P., Runkle, B. R. K., Beckebanze, L., Langer, M., Boike,
892 J., Pfeiffer, E. M., Fedorova, I., Bolshianov, D. Y., Grigoriev, M. N., and Kutzbach, L.: A long-
893 term (2002 to 2017) record of closed-path and open-path eddy covariance CO2 net ecosystem
894 exchange fluxes from the Siberian Arctic, Earth System Science Data, 11, 221-240, doi:
895 10.5194/essd-11-221-2019, 2019.

896 Hu, F. S., Higuera, P. E., Duffy, P., Chipman, M. L., Rocha, A. V., Young, A. M., Kelly, R., and
897 Dietze, M. C.: Arctic tundra fires: natural variability and responses to climate change, Frontiers
898 in Ecology and the Environment, 13, 369-377, doi: 10.1890/150063, 2015.

899 Hubberten, H.-W., Wagner, D., Pfeiffer, E.-M., Boike, J., and Gukov, A. Y.: The Russian-
900 German research station samoylov, Lena delta -A key site for polar research in the Siberian
901 arctic, Polarforschung, 2006.

902 Jorgenson, M. T.: Hierarchical organisation of ecosystems at multiple spatial scales on the
903 Yukon-Kuskokwim Delta, Alaska, USA, Arctic Antarctic and Alpine Research, 32, 221-239, doi
904 10.2307/1552521, 2000.

905 Juhls, B., Antonova, S., Angelopoulos, M., Bobrov, N., Grigoriev, M., Langer, M., Maksimov, G.,
906 Miesner, F., and Overduin, P. P.: Serpentine (Floating) Ice Channels and their Interaction with
907 Riverbed Permafrost in the Lena River Delta, Russia, *Frontiers in Earth Science*, 9, 689941, doi:
908 10.3389/feart.2021.689941, 2021.

909 Kienast, F. and Tsherkasova, J.: Comparative botanical recent-studies in the Lena River Delta
910 [Field Report], Alfred Wegener Institute, Germany, 2001.

911 Landgraf, N., Shevtsova, I., Pflug, B., and Heim, B. .: Sentinel-2 derived central Lena Delta land
912 cover classification, PANGAEA [dataset], <https://doi.pangaea.de/10.1594/PANGAEA.945057>,
913 2022a.

914 Landgraf, N., Shevtsova, I., Pflug, B., and Heim, B.: Raster file with assigned land cover classes
915 and ESRI polygon shape file training classes representing different vegetation composition,
916 PANGAEA [dataset], <https://doi.pangaea.de/10.1594/PANGAEA.945056>, 2022b.

917 Landgraf, N., Shevtsova, I., Pflug, B., and Heim, B.: 23 true Elementary Sampling Units (ESUs)
918 set in the Lena Delta representing the LD18 vegetation plots, PANGAEA [dataset],
919 <https://doi.pangaea.de/10.1594/PANGAEA.945055>, 2022c.

920 Landgraf, N., Shevtsova, I., Pflug, B., and Heim, B.: 69 pseudo Elementary Sampling Units
921 (ESUs) set in the Lena Delta derived with expert knowledge, PANGAEA [dataset],
922 <https://doi.pangaea.de/10.1594/PANGAEA.945054>, 2022d.

923 Lantz, T. C., Kokelj, S. V., and Fraser, R. H.: Ecological recovery in an Arctic delta following
924 widespread saline incursion, *Ecological Applications*, 25, 172-185, doi: 10.1890/14-0239.1,
925 2015.

926 Lisovski, S., Runge, A., Okoth, R. R., Shevtsova, I., and Heim, B.: Lena Delta Land Cover
927 Classification (2018, Sentinel-2), PANGAEA [dataset], doi: 10.1594/PANGAEA.946407, 2022.

928 Lorang, M. S. and Hauer, F. R.: Fluvial geomorphic processes, in: *Methods in stream ecology*,
929 edited by: Hauer, F. R., and Lamberti, G. A., Academic Press/Elsevier, San Diego, 145–168,
930 2006.

931 Macander, M. J., Nelson, P. R., Nawrocki, T. W., Frost, G. V., Orndahl, K. M., Palm, E. C.,
932 Wells, A. F., and Goetz, S. J.: Time-series maps reveal widespread change in plant functional

933 type cover across Arctic and boreal Alaska and Yukon, *Environmental Research Letters*, 17,
934 ARTN 054042, doi: 10.1088/1748-9326/ac6965, 2022.

935 Mauclet, E., Agnan, Y., Hirst, C., Monhonval, A., Pereira, B., Vandeuren, A., Villani, M.,
936 Ledman, J., Taylor, M., Jasinski, B. L., Schuur, E. A. G., and Opfergelt, S.: Changing sub-Arctic
937 tundra vegetation upon permafrost degradation: impact on foliar mineral element cycling,
938 *Biogeosciences*, 19, 2333-2351, doi: 10.5194/bg-19-2333-2022, 2022.

939 Mekonnen, Z. A., Riley, W. J., Berner, L. T., Bouskill, N. J., Torn, M. S., Iwahana, G., Breen, A.
940 L., Myers-Smith, I. H., Criado, M. G., Liu, Y. L., Euskirchen, E. S., Goetz, S. J., Mack, M. C., and
941 Grant, R. F.: Arctic tundra shrubification: a review of mechanisms and impacts on ecosystem
942 carbon balance, *Environmental Research Letters*, 16, 053001, doi: 10.1088/1748-9326/abf28b,
943 2021.

944 Montgomery, D. R.: Process domains and the river continuum, *Journal of the American Water*
945 *Resources Association*, 35, 397-410, doi: 10.1111/j.1752-1688.1999.tb03598.x, 1999.

946 Morgenstern, A., Grosse, G., and Schirrmeyer, L.: Genetic, morphological, and statistical
947 characterization of lakes in the permafrost-dominated Lena Delta, Ninth International
948 Conference on Permafrost, 2008.

949 Morgenstern, A., Grosse, G., Gunther, F., Fedorova, I., and Schirrmeyer, L.: Spatial analyses
950 of thermokarst lakes and basins in Yedoma landscapes of the Lena Delta, *Cryosphere*, 5, 849-
951 867, doi:10.5194/tc-5-849-2011, 2011.

952 Morgenstern, A., Overduin, P. P., Gunther, F., Stettner, S., Ramage, J., Schirrmeyer, L.,
953 Grigoriev, M. N., and Grosse, G.: Thermo-erosional valleys in Siberian ice-rich permafrost,
954 *Permafrost and Periglacial Processes*, 32, 59-75, doi: 10.1002/ppp.2087, 2021.

955 Morgenstern, A., Ulrich, M., Gunther, F., Roessler, S., Fedorova, I. V., Rudaya, N. A., Wetterich,
956 S., Boike, J., and Schirrmeyer, L.: Evolution of thermokarst in East Siberian ice-rich
957 permafrost: A case study, *Geomorphology*, 201, 363-379, doi:
958 10.1016/j.geomorph.2013.07.011, 2013.

959 Mueller-Bombois, D. and Ellenberg, H.: Aims and methods of vegetation ecology, *Wohn Wiley &*
960 *Sons*, New York, USA1974.

961 Myers-Smith, I. H., Kerby, J. T., Phoenix, G. K., Bjerke, J. W., Epstein, H. E., Assmann, J. J.,
962 John, C., Andreu-Hayles, L., Angers-Blondin, S., Beck, P. S. A., Berner, L. T., Bhatt, U. S.,
963 Bjorkman, A. D., Blok, D., Bryn, A., Christiansen, C. T., Cornelissen, J. H. C., Cunliffe, A. M.,
964 Elmendorf, S. C., Forbes, B. C., Goetz, S. J., Hollister, R. D., de Jong, R., Loranty, M. M.,
965 Macias-Fauria, M., Maseyk, K., Normand, S., Olofsson, J., Parker, T. C., Parmentier, F. J. W.,
966 Post, E., Schaepman-Strub, G., Stordal, F., Sullivan, P. F., Thomas, H. J. D., Tommervik, H.,
967 Treharne, R., Tweedie, C. E., Walker, D. A., Wilmking, M., and Wipf, S.: Complexity revealed in
968 the greening of the Arctic, *Nature Climate Change*, 10, 106-117, doi: 10.1038/s41558-019-0688-
969 1, 2020.

970 Naiman, R. J., Melillo, J. M., and Hobbie, J. E.: Ecosystem Alteration of Boreal Forest Streams
971 by Beaver (*Castor-Canadensis*), *Ecology*, 67, 1254-1269, doi: 10.2307/1938681, 1986.

972 Nitzbon, J., Westermann, S., Langer, M., Martin, L. C. P., Strauss, J., Laboor, S., and BOike, J.:
973 Fast response of cold ice-rich permafrost in northeast Siberia to a warming climate, *Nature*
974 *Communications*, 11, 2201, doi: 10.1038/s41467-020-15725-8, 2020.

975 Nitze, I. and Grosse, G.: Detection of landscape dynamics in the Arctic Lena Delta with
976 temporally dense Landsat time-series stacks, *Remote Sensing of Environment*, 181, 27-41, doi:
977 10.1016/j.rse.2016.03.038, 2016.

978 Obu, J., Westermann, S., Barboux, C., Bartsch, A., Delaloye, R., Grosse, G., Heim, B.,
979 Hugelius, G., Irrgang, A., Kääh, A. M., Kroisleitner, C., Matthes, H., Nitze, I., Pellet, C., Seifert,
980 F. M., Strozzi, T., Wegmüller, U., Wiczorek, M., and Wiesmann, A.: ESA permafrost Climate
981 Change Initiative (permafrost_cci): Permafrost extent for the Northern Hemisphere, v2.0
982 [dataset], <https://doi.org/10.5285/28E889210F884B469D7168FDE4B4E54F>, 2020.

983 Overeem, I., Nienhuis, J. H., and Piliouras, A.: Ice-dominated Arctic deltas, *Nature Reviews*
984 *Earth & Environment*, 3, 225-240, doi: 10.1038/s43017-022-00268-x, 2022.

985 Overland, J., Dunlea, E., Box, J. E., Corell, R., Forsius, M., Kattsov, V., Olseng, M. S., Pawlak,
986 J., Reiersen, L. O., and Wang, M. Y.: The urgency of Arctic change, *Polar Science*, 21, 6-13,
987 doi: 10.1016/j.polar.2018.11.008, 2019.

988 Pickett, S. T. A., Kolasa, J., Armesto, J. J., and Collins, S. L.: The Ecological Concept of
989 Disturbance and Its Expression at Various Hierarchical Levels, *Oikos*, 54, 129-136, doi:
990 10.2307/3565258, 1989.

991 Piliouras, A. and Rowland, J. C.: Arctic River Delta Morphologic Variability and Implications for
992 Riverine Fluxes to the Coast, *Journal of Geophysical Research-Earth Surface*, 125, ARTN
993 e2019JF005250, doi: 10.1029/2019JF005250, 2020.

994 Pisaric, M. F. J., Thienpont, J. R., Kokelj, S. V., Nesbitt, H., Lantz, T. C., Solomon, S., and Smol,
995 J. P.: Impacts of a recent storm surge on an Arctic delta ecosystem examined in the context of
996 the last millennium, *Proceedings of the National Academy of Sciences of the United States of*
997 *America*, 108, 8960-8965, doi: 10.1073/pnas.1018527108, 2011.

998 Raynolds, M. K., Walker, D. A., Balsler, A., Bay, C., Campbell, M., Cherosov, M. M., Daniels, F.
999 J. A., Eidesen, P. B., Emiokhina, K. A., Frost, G. V., Jedrzejek, B., Jorgenson, M. T., Kennedy,
1000 B. E., Kholod, S. S., Lavrinenko, I. A., Lavrinenko, O. V., Magnusson, B., Matveyeva, N. V.,
1001 Metusalemsson, S., Nilsen, L., Olthof, I., Pospelov, I. N., Pospelova, E. B., Pouliot, D.,
1002 Razzhivin, V., Schaepman-Strub, G., Sibik, J., Telyatnikov, M. Y., and Troeva, E.: A raster
1003 version of the Circumpolar Arctic Vegetation Map (CAVM), *Remote Sensing of Environment*,
1004 232, ARTN 111297, doi: 10.1016/j.rse.2019.111297, 2019.

1005 Romanovskii, N. N. and Hubberten, H. W.: Results of permafrost modelling of the lowlands and
1006 shelf of the Laptev Sea region, Russia, *Permafrost and Periglacial Processes*, 12, 191-202, doi:
1007 10.1002/ppp.387, 2001.

1008 Rossger, N., Sachs, T., Wille, C., Boike, J., and Kutzbach, L.: Seasonal increase of methane
1009 emissions linked to warming in Siberian tundra, *Nature Climate Change*, 12, 1031-+, doi:
1010 10.1038/s41558-022-01512-4, 2022.

1011 Runge, A., Fuchs, M., Shevtsova, I., Landgraf, N., Heim, B., Herzsuh, U., and Grosse, G.:
1012 Hyperspectral field spectrometry of Arctic vegetation units in the central Lena Delta [dataset],
1013 <https://doi.org/10.1594/PANGAEA.945982>, 2022.

1014 Sachs, T., Wille, C., Boike, J., and Kutzbach, L.: Environmental controls on ecosystem-scale
1015 CH₄ emission from polygonal tundra in the Lena River Delta, Siberia, *Journal of Geophysical*
1016 *Research-Biogeosciences*, 113, ArtN G00a03, doi: 10.1029/2007jg000505, 2008.

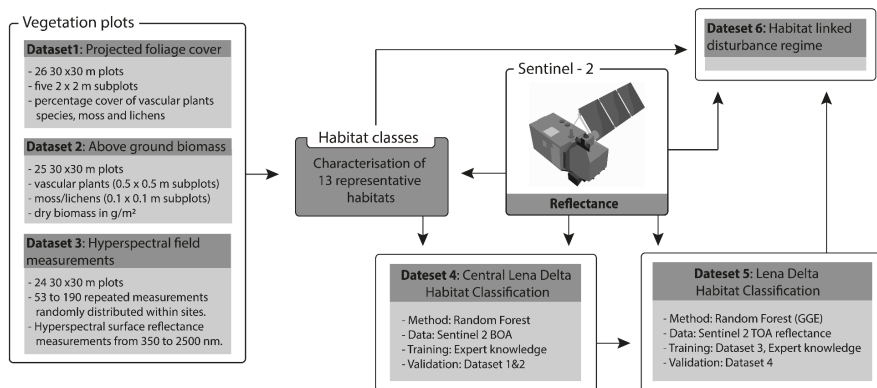
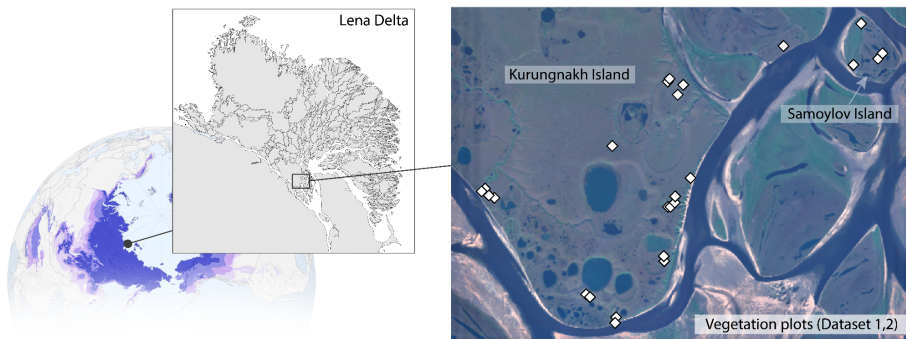
1017 Schirrmeyer, L., Grosse, G., Schwamborn, G., Andreev, A. A., Meyer, H., Kunitsky, V. V.,
1018 Kuznetsova, T. V., Dorozhkina, M. V., Pavlova, E. Y., Bobrov, A. A., and Oezen, D.: Late
1019 Quaternary History of the Accumulation Plain North of the Chekanovsky Ridge (Lena Delta,

- 1020 Russia): A Multidisciplinary Approach, *Polar Geography*, 27, 277-319, doi: 10.1080/789610225,
1021 2003.
- 1022 Schirrmeister, L., Grosse, G., Schnelle, M., Fuchs, M., Krbetschek, M., Ulrich, M., Kunitsky, V.,
1023 Grigoriev, M., Andreev, A., Kienast, F., Meyer, H., Babiy, O., Klimova, I., Bobrov, A., Wetterich,
1024 S., and Schwamborn, G.: Late Quaternary paleoenvironmental records from the western Lena
1025 Delta, Arctic Siberia, *Palaeogeography Palaeoclimatology Palaeoecology*, 299, 175-196, doi:
1026 10.1016/j.palaeo.2010.10.045, 2011.
- 1027 Schneider, J., Grosse, G., and Wagner, D.: Land cover classification of tundra environments in
1028 the Arctic Lena Delta based on Landsat 7 ETM+ data and its application for upscaling of
1029 methane emissions, *Remote Sensing of Environment*, 113, 380-391, doi:
1030 10.1016/j.rse.2008.10.013, 2009.
- 1031 Schwamborn, G., Rachold, V., and Grigoriev, M. N.: Late Quaternary sedimentation history of
1032 the Lena Delta, *Quaternary International*, 89, 119-134, doi: 10.1016/S1040-6182(01)00084-2,
1033 2002.
- 1034 Schwamborn, G., Schirrmeister, L., Mohammadi, A., Meyer, H., Kartoziia, A., Maggioni, F., and
1035 Strauss, J.: Fluvial and permafrost history of the lower Lena River, north-eastern Siberia, over
1036 late Quaternary time, *Sedimentology*, 70, 235-258, doi: 10.1111/sed.13037, 2023.
- 1037 Serreze, M. C. and Barry, R. G.: Processes and impacts of Arctic amplification: A research
1038 synthesis, *Global and Planetary Change*, 77, 85-96, doi: 10.1016/j.gloplacha.2011.03.004,
1039 2011.
- 1040 Shevtsova, I., Laschinskiy, N., Heim, B., and Herzs Schuh, U.: Foliage projective cover of 26
1041 vegetation sites of central Lena Delta from 2018 [dataset],
1042 <https://doi.pangaea.de/10.1594/PANGAEA.935875>, 2021a.
- 1043 Shevtsova, I., Heim, B., Runge, A., Fuchs, M., Melchert, J., and Herzs Schuh, U.: Total above-
1044 ground biomass of 25 vegetation sites of central Lena Delta from 2018 [dataset],
1045 <https://doi.pangaea.de/10.1594/PANGAEA.935923>, 2021b.
- 1046 Stanford, J. A., Lorang, M. S., and Hauer, F. R.: The shifting habitat mosaic of river ecosystems,
1047 *SIL Proceedings*, 1922-2010, 29, 123-136, doi: 10.1080/03680770.2005.11901979, 2005.

- 1048 Sweeney, C., Chatterjee, A., Wolter, S., McKain, K., Bogue, R., Conley, S., Newberger, T., Hu,
1049 L., Ott, L., Poulter, B., Schiferl, L., Weir, B., Zhang, Z., and Miller, C. E.: Using atmospheric
1050 trace gas vertical profiles to evaluate model fluxes: a case study of Arctic-CAP observations and
1051 GEOS simulations for the ABoVE domain, *Atmospheric Chemistry and Physics*, 22, 6347-6364,
1052 doi: 10.5194/acp-22-6347-2022, 2022.
- 1053 Ulrich, M., Grosse, G., Chabrillat, S., and Schirrmeister, L.: Spectral characterization of
1054 periglacial surfaces and geomorphological units in the Arctic Lena Delta using field spectrometry
1055 and remote sensing, *Remote Sensing of Environment*, 113, 1220-1235, doi:
1056 10.1016/j.rse.2009.02.009, 2009.
- 1057 van Everdingen, R. O.: Multi-language glossary of permafrost and related ground-ice terms,
1058 Arctic Institute of North America University of Calgary, Calgary, Canada 1998.
- 1059 Veremeeva, A. and Gubin, S.: Modern Tundra Landscapes of the Kolyma Lowland and their
1060 Evolution in the Holocene, *Permafrost and Periglacial Processes*, 20, 399-406, doi:
1061 10.1002/ppp.674, 2009.
- 1062 Vulis, L., Tejedor, A., Zaliapin, I., Rowland, J. C., and Foufoula-Georgiou, E.: Climate
1063 Signatures on Lake And Wetland Size Distributions in Arctic Deltas, *Geophysical Research*
1064 *Letters*, 48, ARTN e2021GL094437, doi: 10.1029/2021GL094437, 2021.
- 1065 Walker, H. J.: Arctic deltas, *Journal of Coastal Research*, 14, 718–738, 1998.
- 1066 Whitaker, R. H. and Woodwell, G. M.: Dimension, and Production Relations of Trees and
1067 Shrubs in the Brookhaven Forest, New York., *Journal of Ecology*, 56, 1-25, doi: 10.1038/2325,
1068 1968.
- 1069 Zibulski, R., Herzsuh, U., and Pestryakova, L. A.: Vegetation patterns along micro-relief and
1070 vegetation type transects in polygonal landscapes of the Siberian Arctic, *Journal of Vegetation*
1071 *Science*, 27, 377-386, doi: 10.1111/jvs.12356, 2016.
- 1072

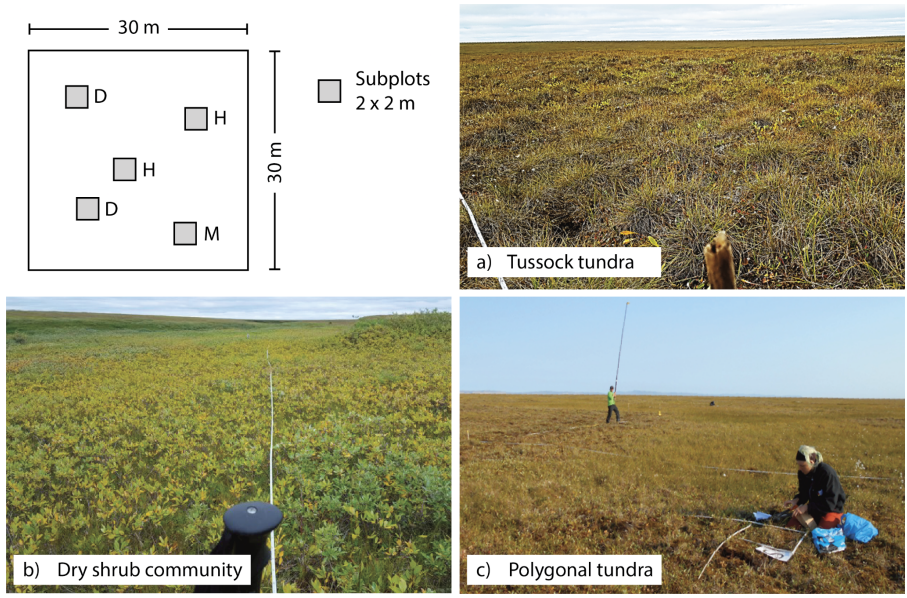
1073 **Figures**

1074



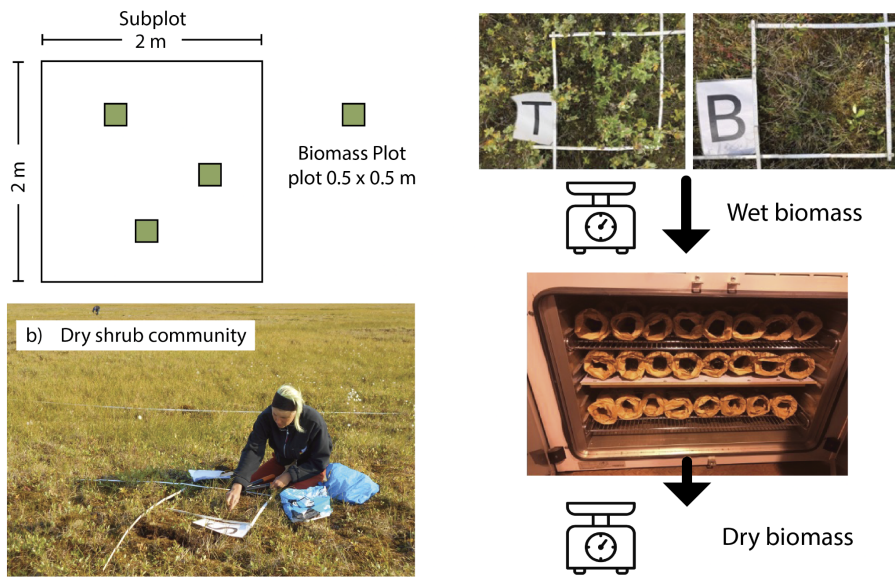
1075

1076 Figure 1: Geographic location of the Lena Delta in the Russian High Arctic (72.91°N, 126.90°E)
 1077 and a Sentinel-2 RGB image (August 2018, bands 4-3-2) of the central Lena Delta showing the
 1078 areas of the 26 vegetation plots where foliage projective cover and above ground biomass was
 1079 determined. Panarctic overview map shows permafrost extent (colour scale indicates
 1080 permafrost extent from continuous (dark purple) to isolated (light purple) (Obu et al., 2020). The
 1081 grey-coloured Lena Delta land map created with Sentinel-1 water mask from Juhls et al. (2021).
 1082 Bottom: Dataset characteristics and methodological links between the different datasets.



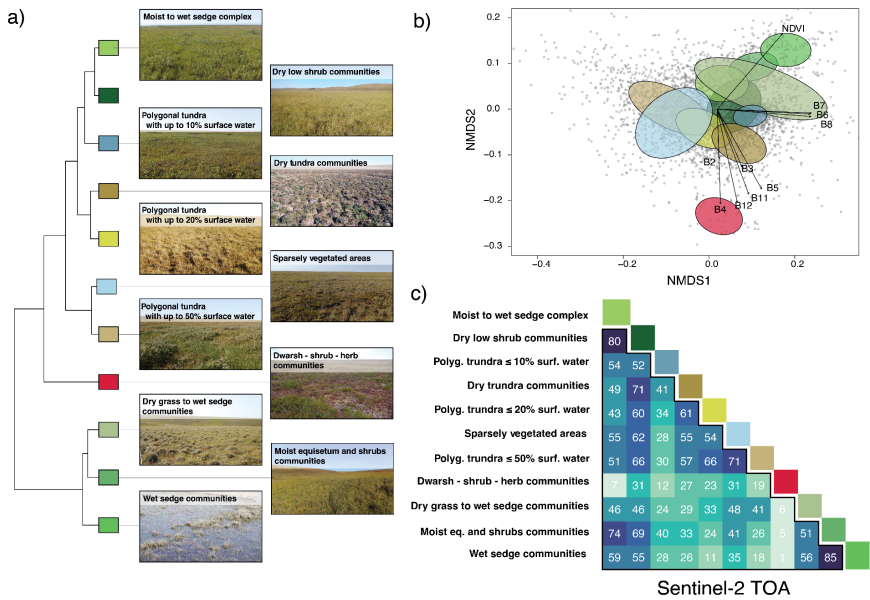
1083

1084 Figure 2. Vegetation plots (30 x 30 m) were established in different vegetation types across the
 1085 central Lena Delta. For subplots (2 x 2 m), the projective vegetation cover was recorded and
 1086 labeled according to vegetation and moisture properties (H-Type: homogeneous, M-Type:
 1087 moist, D-Type: dry). Figures illustrate example plots in a) tussock tundra (VP14), b) dry shrub
 1088 communities (VP05), c) polygonal tundra (VP13). Photos: AWI.



1089

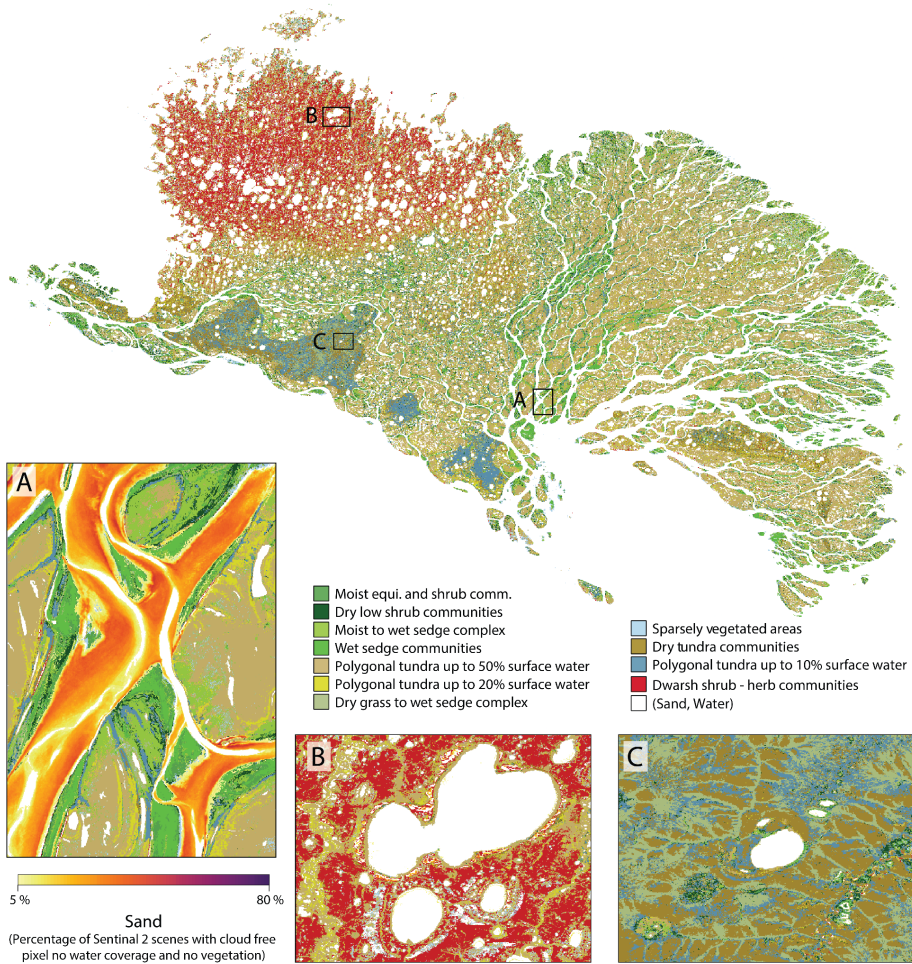
1090 Figure 3. Biomass was sampled in subplots of 0.5 x 0.5 m (and 0.1 x 0.1 m for moss and
 1091 lichens) distributed within the 2 x 2 m subplots described in Figure 2. Collected plants were
 1092 weighted (wet biomass), dried in an oven and again weighted (dry biomass). Fotos: AWI.



1093

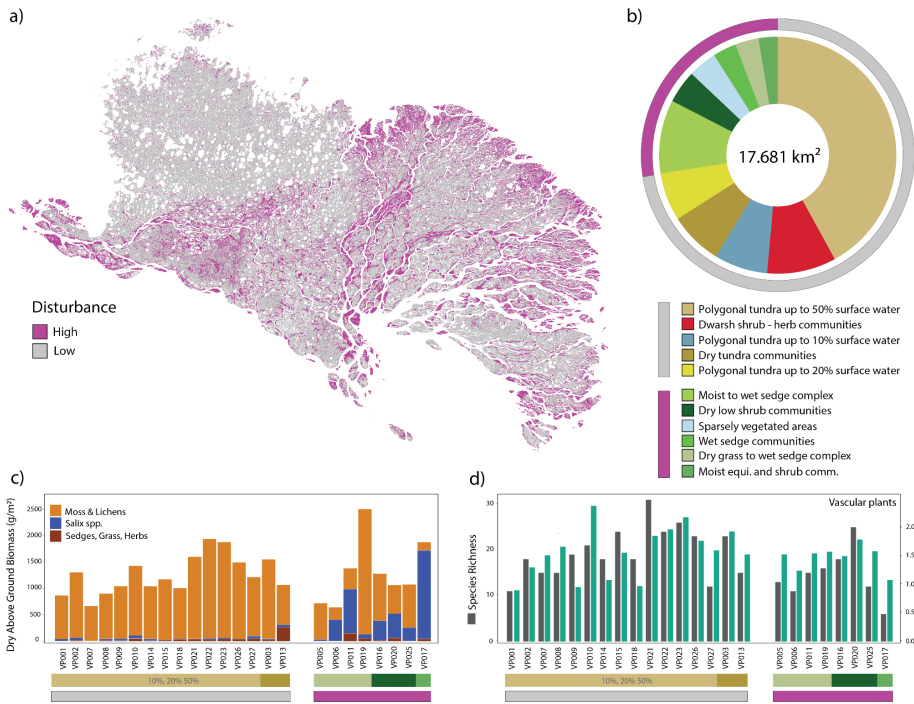
1094 Figure 4: Similarity of habitat classes based on Sentinel-2 spectral reflectance and NDVI values.
 1095 The dendrogram in panel a) indicates the multidimensional hierarchical similarity of the classes
 1096 based on Sentinel-2 top of atmosphere reflectance (bands 2-8, 10-12, and NDVI). Panel b)
 1097 shows the location of the habitat classes within a two-dimensional NMDS space. The arrows
 1098 with the Sentinel-2 bands and NDVI indicate the correlation of these variables across the two
 1099 axes. The lower matrix of panel c) depicts the calculated percentage overlap of 3,500 pixels
 1100 (grey dots in panel b) across the two NMDS axes of panel b).

1101



1102

1103 Figure 5: Lena Delta habitat classes (Dataset 5). The entire Lena Delta on the left with three
 1104 regional examples, showing (A) the seasonal sand probability and (B, C) regional examples of the
 1105 habitat classes.



1106

1107 Figure 6: Habitat linked disturbance regimes across the Lena Delta. The map (a) includes all
 1108 vegetated areas (excluding water and sand). The pie chart (b) shows the contribution of
 1109 vegetated classes across the Lena Delta grouped by high and low disturbance regimes. The
 1110 bottom panels show c) the measured dry above ground biomass (Dataset 2) and d) the species
 1111 richness and Shannon index (from Dataset 1) of the vegetation plots for different habitat classes
 1112 and disturbance regimes.

1113

1114 **Tables**

1115 Table 1: Habitat classes, descriptions as well as methods used to characterize the distinct
 1116 habitats. In-situ vegetation plot numbers correspond to the vegetation plots of Dataset 1 and 2
 1117 (see also Table S1, S2, S3).

1118

Habitat types	Description	Method
Moist <i>Equisetum</i> and shrubs	<i>Equisetum</i> and shrub communities form a early-to-middle successional stage growing on the active floodplain. Low moss contribution	In-situ vegetation plot (VP17); extended to representative larger polygon shape files using field knowledge.
Dry shrub communities	Patch forming shrub communities dominated by dwarf willow (<i>Salix</i>) thickets, frequently occurring on dry elevated areas on floodplains and stream floodplains and in topographically sheltered areas below basin and valley rims. Low moss contribution	In-situ vegetation plots (VP04, VP16); extended to representative larger polygon shape files using field knowledge.
Polygonal tundra complex up to <ul style="list-style-type: none"> - 10% - 20% - 50% surface water (3 distinct classes)	Mature-state plant communities dominated by sedge, moss and herb species. Sparse vascular plant coverage (dwarf willows, dwarf birches) on thick continuous moss cover. Occurring on the plateaus of the ice-rich holocene and pleistocene terraces, and at the bottom of alases. Intersected by intra- and interpolygonal ponds resulting in up to 10%, 20%, 50% surface water contribution.	In-situ vegetation plots (VP01, VP02, VP07, VP08, VP14, VP15, VP18, VP21, VP22, VP23, VP26, VP27); extended to representative larger polygon shape files using field knowledge. The different surface water contributions were defined based on the result from unsupervised classification.

<p>Dry grass to wet sedge communities</p>	<p>These early-to-middle successional plant communities cover unstable valley slopes and a young drained lake basin, they are mostly composed of sedges and grasses, but also willows (<i>Salix</i>) are part of this habitat.</p>	<p>In-situ vegetation plots (VP05, VP06, VP11, VP19, VP20); extended to representative larger polygon shape files using field knowledge.</p>
<p>Dry tundra communities</p>	<p>The mature-state dry tundra communities represent the zonal tundra type, one subclass is dominated by tussock forming <i>Eriophorum</i> and the other by less tussock forming dry-herb communities, dominated by <i>Dryas</i>. Occurring on well-drained slopes of valleys and alases, and other well-drained areas on the terraces. High moss contribution</p>	<p>In-situ vegetation plots (VP03, VP13) extended to representative, larger polygon shape files using field knowledge (including 'dry tundra communities type tussock' and 'dry tundra communities').</p>
<p>Moist to wet sedge communities</p>	<p>These mid to advanced successional plant communities occur on moist to water-logged soils characteristically mostly in topographic depressions on the floodplains, in valleys and alases. They constitute the rims of the wetland areas on the floodplains in more dynamic parts the moss ground cover is missing.</p>	<p>Polygon shape files derived from high resolution satellite image and ESRI GE with regional expert knowledge. No vegetation plots (too wet).</p>
<p>Wet sedge communities</p>	<p>These mid to advanced successional plant communities occur at permanently wet sites with stagnant water in the topographic depressions and are typical for wetland areas on the floodplains. In more dynamic parts the moss ground cover is missing.</p>	<p>Polygon shape files derived from high resolution satellite image and ESRI GE with regional expert knowledge. No vegetation plots (too wet).</p>

Sparse vegetated areas	These early successional plant communities are characterized by low vegetation establishment and coverage. No to low moss contribution	Defined based on the result from unsupervised classification, polygon shape files. No vegetation plots.
Barren/Sand	Representing the wide-open sand flats of the floodplain and barren ground on valley slopes or along cliffs. In a few cases, this class represents vegetation-free bedrock outcrops.	Threshold using high reflectance in S2-band 2 blue.
Water	Represents all surface water bodies in the delta: the Lena River with river branches, streams, lakes and large ponds.	Threshold using low reflectance in S2-band 8 NIR.

1119

1120 Table 2: Habitat class and description of disturbance regimes and the component stand
 1121 structure in form of contributions of vascular plants, and moss to total biomass. * (Driscoll and
 1122 Hauer, 2019; Stanford et al., 2005), ** (Lorang and Hauer, 2006).

Habitat class	Disturbance regime	Stand structure
Moist <i>Equisetum</i> and shrubs	High; regular (annually), predicted - spring floodings, - shifting habitat * - advanced-stage regeneration **	high vascular plant growth, low abundance of moss & lichens.
Dry shrub communities	High; mixed disturbance types: -regular spring floodings -rapid thaw processes (permafrost degradation) - shifting habitat - advanced-stage regeneration	high vascular plant growth, low abundance of moss.
Polygonal tundra complex	Low; mixed disturbance types - low for most of the habitat, except for actively eroding shores of ponds and channels - mature-state plant community	low vascular plant growth, high abundance of moss.
Dry grass to wet sedge communities	High; mixed disturbance types: - regular spring floodings - rapid thaw processes (permafrost degradation) - shifting habitat	high vascular plant biomass, low abundance of moss.

	- advanced-stage regeneration	
Dry tundra communities	<p>Low; mixed disturbance types</p> <ul style="list-style-type: none"> - low for most of the habitat - mature-state plant community 	<p>low vascular plant biomass</p> <p>high abundance of moss.</p>
Moist to wet sedge communities	<p>High; mixed disturbance types:</p> <ul style="list-style-type: none"> - regular spring floodings - rapid thaw processes (permafrost degradation) - shifting habitat - mid to advanced-stage regeneration 	<p>high vascular plant biomass Almost impossible to measure in-situ biomass (wet conditions and difficult access).</p>
Wet sedge communities	<p>High; mixed disturbance types:</p> <ul style="list-style-type: none"> - regular spring floodings - rapid thaw processes (permafrost degradation) - shifting habitat - mid to advanced-stage regeneration 	<p>high vascular plant biomass. Almost impossible to measure in-situ biomass (wet conditions and difficult access).</p>
Dwarf shrub herb communities	<p>Low; mixed disturbance types</p> <ul style="list-style-type: none"> - low for most of the habitat - mature-state plant community 	<p>low vascular plant biomass, high abundance of moss.</p>

<p>Sparsely vegetated areas</p>	<p>Very high; mixed disturbance types</p> <ul style="list-style-type: none"> - regular spring floodings - rapid thaw processes (permafrost degradation) - shifting habitat - early-stage regeneration 	<p>lowest vascular plant biomass, no moss.</p>
<p>Sand banks/barren</p>	<p>Very high: mixed disturbance types</p> <ul style="list-style-type: none"> - regular spring floodings - rapid thaw processes (permafrost degradation) - shifting habitat - no regeneration 	<p>Barren, constant shifting of sediments and movement of soils.</p>

1123